

PALEOCURRENT ANALYSIS AND PALEOENVIRONMENTAL
INTERPRETATION OF THE ABO FORMATION, ABO CANYON AREA,
VALENCIA, TORRANCE, AND SOCORRO COUNTIES, NEW MEXICO

by

Kenneth Ray Lemley

NMIMTAR - International
Resource and Gender Center

Submitted in partial fulfillment of the requirements for
the degree of Master of Science in Geology

New Mexico Institute of Mining and Technology

Socorro, New Mexico

June, 1984

TABLE OF CONTENTS

ACKNOWLEDGMENTS..... vi

ABSTRACT..... vii

CHAPTER 1: INTRODUCTION..... 1

 Purpose..... 1

 Background..... 1

 Methodology..... 2

 Previous Work..... 6

CHAPTER 2: GENERAL GEOLOGY OF ABO CANYON..... 9

 Introduction..... 9

 Geologic Setting..... 9

 Stratigraphy..... 9

CHAPTER 3: EVALUATION OF STATISTICAL
 TECHNIQUES USED FOR PALEOCURRENT
 DATA ANALYSIS 13

 Introduction..... 13

 Procedure..... 13

 Statistical Treatment..... 16

 Tests of Significance..... 21

CHAPTER 4: DEPOSITIONAL ENVIRONMENT..... 24

 Introduction..... 24

 Fluvial Models..... 24

 Channel sand deposits..... 25

 Overbank deposits..... 25

Fluvial Parameters and Channel	
characteristics.....	26
channel width/ channel depth ratio.....	28
Sinuosity.....	29
Silt and Clay percentage.....	31
Discharge.....	33
Velocity.....	33
Water Depth.....	34
Froude Number.....	34
Meander Wavelength.....	35
Meander Amplitude.....	35
Mean Radius of curvature.....	36
Channel Gradient.....	36
Valley Gradient.....	37
Mean Annual Flood.....	37
Ephemeral flow verses Perennial flow.....	37
Paleocurrent Analysis.....	38
Lower Arkose Unit.....	39
Middle Mudstone Unit.....	39
Upper Sandstone Unit.....	41
Fluvial parameter analysis.....	46
Regional Depositional System.....	51

CHAPTER 5: STATISTICAL COMPARISON OF SCALED PALEOCURRENT STRUCTURES.....	53
Introduction.....	53
Small vs. medium vs. large scale paleocurrent indicators within a single unit and between units of similar paleoenvironment.....	54
Small scale.....	54
Medium scale.....	54
Large scale.....	55
Conclusions.....	55
Channel sand deposits vs. Overbank deposits.....	56
Comparison of a channel sand deposit and it's adjacent overbank deposit.....	57
APPENDIX.....	59
BIBLIOGRAPHY.....	84

LIST OF PHOTOS

Photo 1. View looking west of lithologic units
AS119A and AS119B..... 43

Photo 2. View looking west of lithologic units
AS119A and AS119C..... 43

LIST OF FIGURES

Figure 1. Distribution of Late Paleozoic landmasses.....	3
Figure 1a. Study area location map.....	4
Figure 2. Abo Type Section.....	12
Figure 3. Vector strength vs. Standard deviation.....	19
Figure 4. Sketch to define terms used in describing characteristics of a meandering channel.....	27
Figure 5. Fluvial parameters vs. relative stratigraphic position.....	48

LIST OF TABLES

Table 1. Equations used in the calculation of various fluvial parameters.....	30
Table 2. Sediment transport in stable alluvial channels.....	32
Table 3. Statistics calculated for each lithologic unit studied.....	40
Table 4. Fluvial parameter results as calculated from equations given in table 1.....	47

ACKNOWLEDGMENTS

I am very grateful to my thesis advisor, Dr. John MacMillan, for his help and guidance during this study.

This thesis was funded by the State Mining and Mineral Resources Research Institute. I am grateful for the teaching assistantship granted to me by the New Mexico Institute of Mining and Technology without which I would not have been able to finish school.

Many thanks to my friends, colleagues and especially my professors, all of whom contributed, in many different ways, to the final completion of this thesis.

ABSTRACT

A total of 206 paleocurrent directions from 12 different sedimentary lithologic units of the Abo Formation in east-central New Mexico were collected and analyzed. The direction of the resultant vector (vector mean) as computed for each lithologic unit, range from southwest to northeast with a strong westerly component. Statistical analysis of the paleocurrent data give the following conclusions: a) Large scale paleocurrent structures are less variable than medium scale paleocurrent structures, which are less variable than small scale paleocurrent structures. b) Not enough difference exists in variability between the scaled paleocurrent structures to warrant "weighting" of these structures for analysis. c) Paleocurrents taken from an overbank deposit should not be used to infer the paleocurrent direction of the adjacent river channel, nor be combined with paleocurrent data from the channel.

Analysis of the change in the channel width/channel depth ratio throughout time indicate an upward decrease in sinuosity followed by a dramatic increase. The valley gradient is approximately two times as great as the channel gradient. These, as well as changes in other fluvial parameters, indicate an increase in tectonism of the source area followed by a dramatic decrease. This dramatic decrease in tectonism of the source area may be related to

covering of the source area by the Abo Formation during Early Permian time. A rise in base level, which may be associated with a rise in sea level, is thought to have occurred throughout this time also.

INTRODUCTION

Purpose

The purpose of this thesis is two-fold. The first is to quantitatively determine, where possible, the depositional environment and paleocurrent directions of the Abo Formation in central New Mexico and then utilize this data to place the Abo Formation within the regional depositional setting of central New Mexico. The second purpose is to qualitatively and, if possible, quantitatively determine the statistical validity of small versus medium versus large scale paleocurrent indicators within a particular lithologic unit, between units of similar lithology and between units of differing lithologies and paleoenvironments such as a channel sandstone and its adjacent overbank deposit.

The depositional environment of a particular unit as well as the Abo Formation, in general, is determined through lithologic, stratigraphic, and paleocurrent analysis. Fossil organisms, which occur in the Abo Formation, were not studied for their environmental significance. The majority of lithologic data was taken from the literature and only briefly supplemented where deemed necessary.

Background

The exact age of the Abo Formation is the subject of some controversy (King, R.E., 1945; Kottowski and Stewart, 1970). For the purpose of this thesis the Abo Formation is considered to be both Wolfcampian and Leonardian in age in the study area.

The Abo Formation outcrops as north-south trending belts throughout New Mexico. From the Sangre De Cristo and Nacimiento mountains in the north, southward to the Zuni, Sierra Lucero Mesa, Manzano, Los Pinos, Sacramento, Caballo, and San Andres mountains (Darton, 1928).

Previous work on the Abo red beds indicate a fluvial - alluvial environment (Hatchell, et al., 1982; Needham and Bates, 1943). This is based on stratigraphic relationships, the presence of mud cracks, raindrop imprints, land vertebrate tracks, nonmarine plant imprints, and carbonized land plants; trough-like geometry and lateral discontinuity of many sandstones and conglomerates; the dominance and style of cross-stratification present within the Abo Formation.

Methodology

The Abo Formation was studied in a vertical section approximately 1.5 miles north of the type-section near the town of Scholle, New Mexico (see Figures 1 and 1a). The type-section was unavailable for study because access to private property was denied by the land owners.

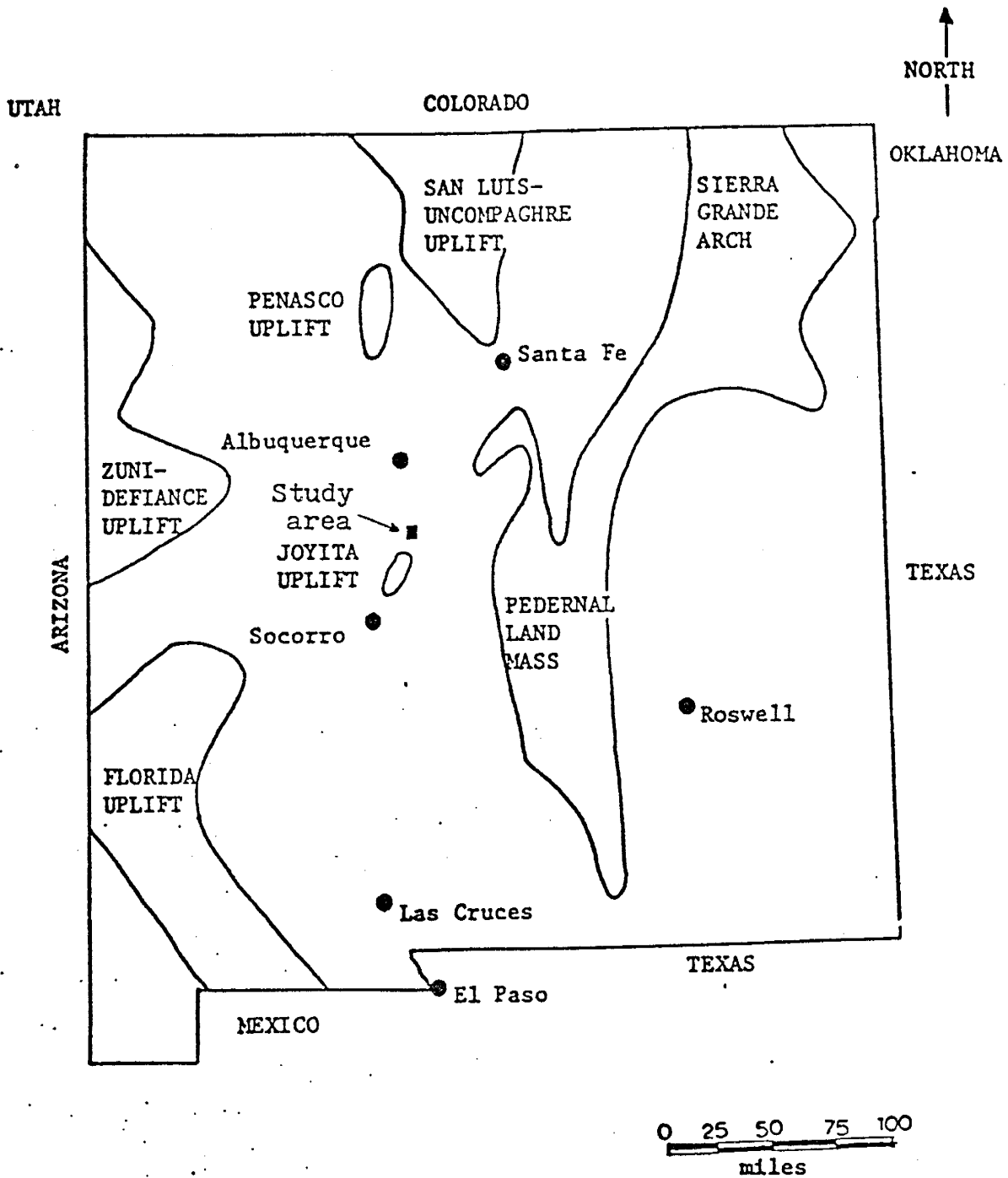


Figure 1. Distribution of Late Paleozoic landmasses (after Kottlowski and Stewart, 1970; McKee, 1967).

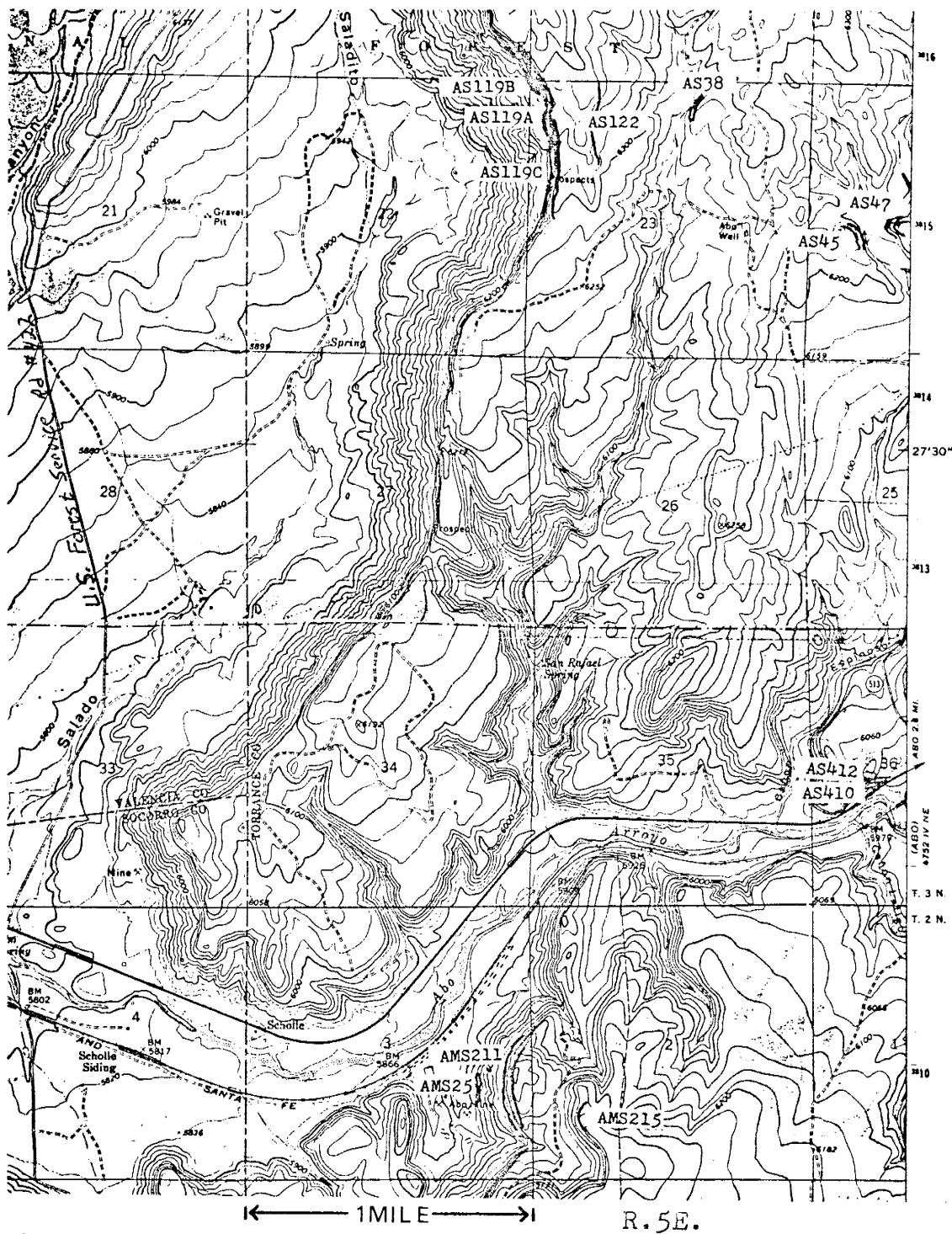


Figure 1a. Study area location map



Most of the previous studies of the Abo Formation neglected quantitative measurements of primary sedimentary structures as an aid in determining depositional environment and source rock location. Instead, previous workers usually concentrated on stratigraphic relationships, texture, and lithology.

At Scholle, New Mexico the lithology was previously described by Needham & Bates (1943) and revised by Hatchell, et al., (1982). The lithologic description was only briefly supplemented where needed.

Where possible, data concerning the channel width and channel depth and the thicknesses of large scale cut-and-fill structures (channel sands) are used to infer gradient, sinuosity and discharge as well as other fluvial parameters of the paleochannels.

Paleocurrent measurements were taken from each available conglomerate, sandstone, siltstone and mudstone unit in the study area. These paleocurrent measurements were then classified on the basis of vertical extent of the set of cross-strata in question, with small scale being less than 10 centimeters, medium scale 10 centimeters to 1 meter, and large scale being greater than 1 meter. The trend and plunge of the dip vector of true bedding was measured at each locality where a paleocurrent measurement was taken. This was done so that the measurements could be rotated back to original horizontality. After rotation the paleocurrent measurements were then plotted on rose diagrams and analyzed using accepted statistical techniques. The results are used

to compare the statistical validity of the various paleocurrent indicators to each other. Changes in source area direction, as well as paleocurrent variability, may indicate the nature and extent of tectonism during deposition of the Abo Formation.

To determine the depositional environment of the Abo Formation its primary sedimentary structures, lithology, and stratigraphy will be compared to modern sediments of known depositional environment.

Previous Work

The Abo was first described and named by Lee and Girty (1909) at Abo Pass, but was not formally defined until 1943 by Needham and Bates. The Abo "red beds" were recognized by N.H. Darton (1928) in his study of the "red beds" of New Mexico. Darton described a facies change from the continental Abo "red beds" of the north to near-shore marine limestones in the Sacramento Mountains to the south.

Needham and Bates (1943) described 914 feet (278.7 meters) of the Abo Formation at Abo Pass, located at the southern edge of the Manzano Mountains along U.S. Highway 60, and thus first formally defined the Abo type-section. They readily recognized the continental origin by the presence of mudcracks, cross-bedding, tracks of land vertebrates, and plant imprints.

Hatchell, et. al., (1982) show a composite section with four partial sections of the Abo Formation at Abo Pass and corrected a stratigraphic error of Needham and Bates (1943). Needham and Bates (1943) included the Meseta Blanca

Sandstone Member of the Yeso Formation with the Abo Formation. Hatchell, et al., (1982) utilized the definition of Northrop and Wood (1946) that the Abo-Yeso contact be drawn below the lowest tangentially cross-bedded sandstone of the Meseta Blanca Sandstone Member. Hatchell, et al., (1982) further suggest that gypsum and salt hopper casts occur immediately above this boundary and should be used to define the Abo-Yeso contact. The author accepts these criteria as a viable way to define the Abo-Yeso contact.

At the type-locality the Abo Formation rests conformably on the Bursum Formation. As will be discussed later this "conformable" contact is the subject of much controversy. Southward in the Joyita Hills, Sacramento Mountains and Oscura Mountains, the Abo-Bursum contact is reported as conformable by Kottowski and Stewart, 1970; Wilpolt and Waneck, 1951; Pray, 1961; Otte, 1959. Bachman (1968) and Thompson (1942) report it as an unconformity in the Oscura and San Andres Mountains. Further south the Bursum Formation is reported to wedge out under the overlying Abo red beds, and thus the Abo intertongues with the Hueco Limestone (Kottowski and Stewart, 1970; Pray, 1961).

Source areas for the Abo Formation have been the subject of many studies (Bachman, 1964; Tonking, 1957; Otte, 1959; Baars, 1961; Pray, 1961; Meyer, 1966; McKee, 1967; Kottowski and Stewart, 1970; LaPoint, 1974). The most common source rock mentioned is the Precambrian granitic

rocks of the Pedernal landmass (see Figure 1). However, Kottowski and Stewart (1970), concluded that the Joyita Hills Precambrian granitic gneiss was a local source for the Abo's red beds of that area. Baars (1961) concludes that the Uncompaghre-San Luis uplift was the source area for the Abo exposed in the area surrounding that uplift. Other workers concluded that the Penasco uplift, Sierra Grande Arch, Zuni-Defiance uplift and Florida uplift were all source areas for the Abo exposed near those uplifts. It is therefore concluded by the author that the various local highlands were the source areas for the spatially adjacent portions of the Abo Formation.

By late Wolfcampian time the Joyita Hills, and most of the southern portion of the Pedernal landmass, were buried by the Abo red beds (Kottowski and Stewart, 1970; Meyer, 1966). This infers a different source for the Abo sediment during Leonardian time.

GENERAL GEOLOGY OF ABO CANYON

Introduction

Abo Canyon is located at the juncture of Torrance, Valencia, and Socorro counties. The study area is limited to sections 2 & 3, T.2N.,R.5E. sections 22, 23 & 24 T.3N., R.5E. The general physiography is one of generally nonresistant shales interbedded with resistant sandstones forming a valley and ridge topography. The maximum relief in the area is 480 feet.

Geologic Setting

Strata in the study area dip 3 to 4 degrees to the southeast (Hatchell, et al., 1982; Myers, 1977). Within the study area, no major folds or faults have been observed or mapped (Myers, 1977). The Abo outcrops in a northeasterly trending belt approximately 4 to 5 miles wide, representing 810 feet (247 meters) of stratigraphic section. The Abo rests conformably on the Bursum Formation of Wolfcampian age, which outcrops to the west. Towards the east, the Abo is conformably overlain by the Meseta Blanca Sandstone Member of the Yeso Formation of Leonardian age.

Stratigraphy

The formations present within the study area, in ascending order, are the Bursum, Abo, and Yeso. The Bursum consists of interbedded limestone, feldspathic sandstone, feldspathic conglomerate, and purplish shale. The upper portions of the Bursum consist of limestones interbedded with crossbedded, reddish feldspathic sandstone (Hatchell, et al., 1982). The Abo-Bursum contact is conformable and

exposed in Canon Solada and along U.S. forest service road 422. Many authors believe, because the base of the Abo occupies scours that erode into the Bursum, that the contact is disconformable (Hatchell, et al., 1982; Needham and Bates, 1943). However, because of the fluvial nature of the Abo which would be expected to cut scours and thus have a lower erosional surface, and the very similar lithologies of the Abo and Bursum, the contact is regarded here as a diastem rather than an unconformity.

The Abo Formation is a series of red colored feldspathic sandstones, conglomerates, and shales. In the vicinity of the type-locality, the Abo can be divided into three units based upon the dominant lithology present. The lower arkose unit consists of feldspathic sandstones and conglomerates 154 feet (47 meters) thick. The top of a prominent sandstone separates the lower arkose unit from the middle mudstone unit. The middle mudstone unit is 531 feet (162 meters) thick and consists dominantly of shales. The base of a prominent sandstone, which caps mesas in the study area, separates the middle mudstone unit from the upper sandstone unit. The upper sandstone unit is 144 feet (44 meters) thick and consists mostly of shales with sandstones being slightly more common in the upper unit than the middle or lower units (Hatchell, et al., 1982).

Thus at the type-locality, shales are the dominant lithology with a sand:shale ratio of approximately 1:4 (Hatchell, et al., 1982). A detailed stratigraphic section of the Abo Formation (from Hatchell, et al., 1982)

is shown in Figure 2.

Conformably overlying the Abo is the Meseta Blanca Sandstone Member of the Yeso Formation. The Meseta Blanca Sandstone Member consists of reddish sandstones with interbedded reddish mudstones. The presence of gypsum and salt hopper casts serves as a useful criterion to define the Abo-Yeso contact (Hatchell, et al., 1982). In the study area the Yeso is 350 feet (107 meters) thick (Myers, 1977).

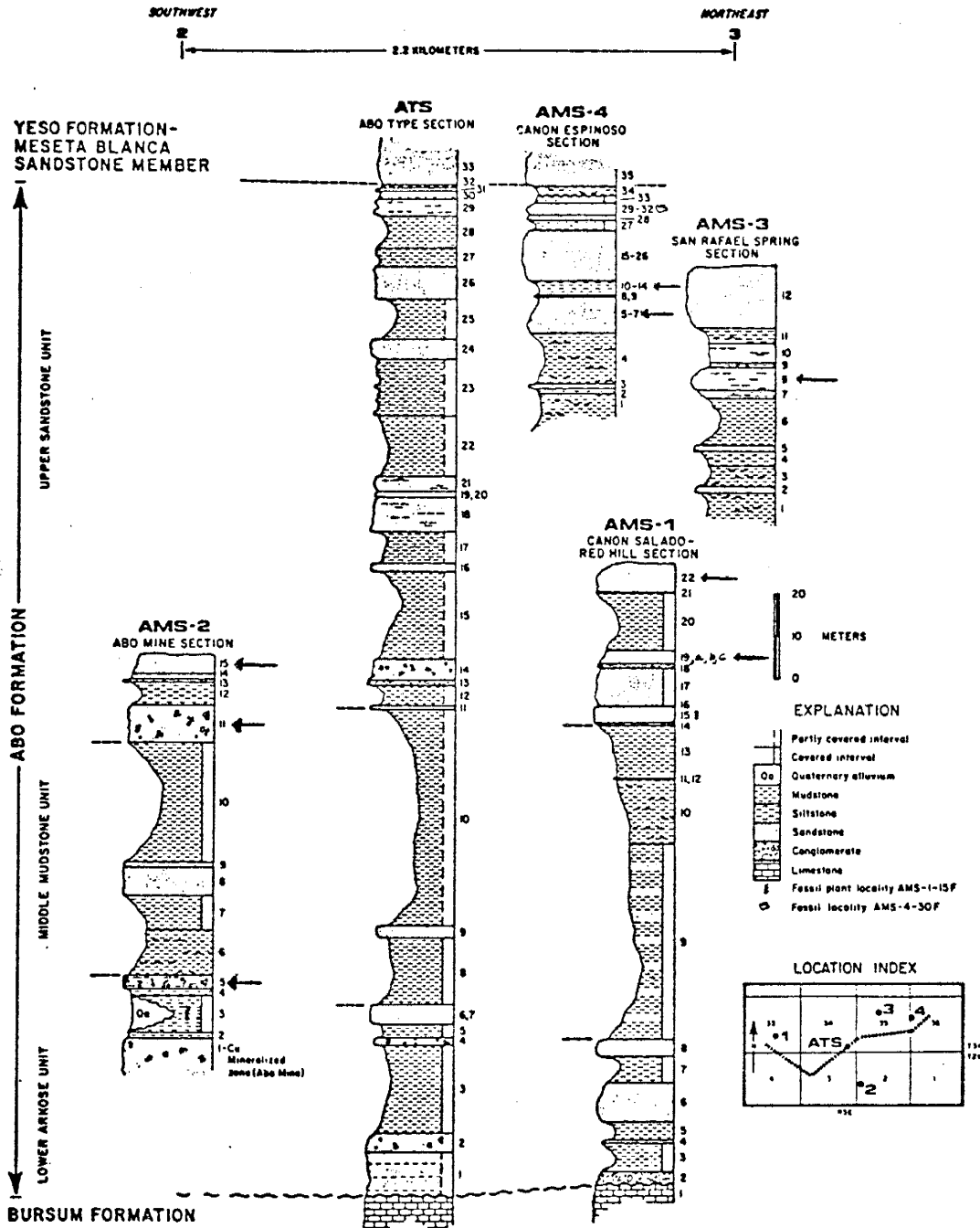


Figure 2. Abo type section showing informal stratigraphic units and Formational boundaries. (taken from Hatchell, Blagbrough, and Hill, 1982). Arrows indicate lithologic units studied.

EVALUATION OF STATISTICAL TECHNIQUES USED FOR PALEOCURRENT
DATA ANALYSIS

Introduction

The Abo Formation contains an abundant and diverse mixture of primary sedimentary structures. These include many varieties of large, medium and small scale sets of cross-stratification, ripple marks, climbing ripples and tool marks. These structures can be used to infer paleocurrent direction, paleoslope, paleogeomorphology, paleotectonic history, depositional environment and character of the depositing medium.

Procedure

A total of 206 paleocurrent measurements of all varieties were taken from 12 outcrops of differing lithologies and depositional environments. These paleocurrent measurements were then classified on the basis of maximum thickness of the set of cross-strata under study. A set was defined by Mckee and Weir (1953) as a group of essentially conformable strata or cross-strata, separated from other sedimentary units by surfaces of erosion, non-deposition, or abrupt change in rock characteristics. This definition is used in this study. Small scale is less than ten centimeters thick, medium scale ranges from ten centimeters to one meter and large scale is greater than one meter. The shape of the set of cross-strata, such as trough, tabular, etc. was recognized but not recorded. Much of the cross-stratification is not

clearly of a single shape category, but a combination of two or more shapes and thus did not lend itself well to classification into trough, tabular, etc.

Paleocurrent measurements were taken by a number of methods depending upon the quality of exposure. In areas of good exposures where a three dimensional view of a particular sedimentary structure was available, the direct measurement of the foreset dip direction and dip angle was possible. In areas of poorer exposure the apparent dip and direction of dip of the foreset bed was taken from two or more surfaces and then plotted on a stereonet to determine the trend and plunge of the foreset bed. In cut and fill structures three measurements of the orientation of the lower erosional surface were taken, plotted on a stereonet and the trend and plunge of the axis of the structure was determined. Stereographic procedures are given in Phillips(1954).

If the precision of the paleocurrent measurement exceeded 10 degrees, then the measurement was not recorded.

In the study area, the strata dip gently to the southeast. Paleocurrent measurements were rotated a set number of degrees equal to that of the plunge of the dip vector of bedding about an axis parallel to the strike of bedding. A computer program written by Sue Daut (1978) and adapted by the author makes this procedure quick and easy. In some instances, original paleocurrent measurements whose plunge was equal to or less than the dip of bedding, could, by computer processing of the data, be "flipped over" to the

opposite quadrant and thus the paleocurrent direction would point in the opposite direction. A field judgment was made on whether or not this would happen. To correct where necessary, the inclination of the lineation was arbitrarily increased until it was greater than the plunge of bedding. Foliations, such as cross-strata, were less susceptible to this type of decision.

After rotation, the data was then grouped into ten degree modes starting at five degrees east of north. The frequency of each mode was then determined and a resulting rose diagram was drawn. The rose diagram was further subdivided on the basis of the scale of the sedimentary structure from which the paleocurrent was measured. Again, computer processing made this procedure quick and easy.

The resulting data was then analyzed using various statistical techniques for comparison.

Statistical Treatment

Various techniques for analyzing directional data exist. Some authors (Griffiths and Rosenfeld, 1953; Gumbel et al, 1953; Watson and Williams, 1956; Dixon and Massey, 1957; Harrison, 1957; Jones, 1968; Miller and Kahn, 1962) suggest the extension of standard properties of a normal distribution (mean, standard deviation, etc.) to directional data. Properties such as mean, standard deviation, and variance for directional data are all critically dependent upon the choice of origin. For example, if north, 0 degrees, is chosen as the origin and we have data at 359 degrees and at 1 degree the mean would be 180 degrees, which is south and opposite of the true sense of direction. The resulting standard deviation and variance would be erroneously high. If east, 90 degrees, were chosen as the origin, the data would convert to 269 degrees and 271 degrees, respectively. The mean would be 270 degrees, the true sense of direction, the standard deviation and variance would then be appropriately small. As a result many authors suggest modified methods for computing the mean, standard deviation and variance for directional data. In 1938, Reiche introduced the concept of the vector mean for analyzing directional data. In computing the vector mean, each datum is treated as a vector with a unit magnitude. The vector mean is the vector

sum of each of the data treated individually or within a class interval as High and Picard (1971) advocate. The vector mean is calculated by the following equation:

$$\text{Tan } \theta = \frac{\sum \text{Sin } @}{\sum \text{Cos } @}$$

where,

θ = azimuth of resultant vector (vector mean)

@ = data azimuth

The magnitude of the resultant vector (R), is given by:

$$R = \left[\sum \sin^2 @ + \sum \cos^2 @ \right]^{1/2}$$

The vector strength (L), is given by:

$$L = R/n$$

where,

n = total number of data measurements

It is empirically obvious that the vector strength would decrease, to a minimum of 0, as the variability of the data increases, and would increase to a maximum of 1 as the variability of the data decreases. Two populations with differing variabilities may have the same resultant vector magnitude (R) but not the same vector strength (L). For these reasons, the vector strength (L) is a better measure of the variability of the data than the magnitude of the resultant vector (R).

Figure 3 shows a plot of vector strength (L) vs. standard deviation. A very good correlation exists between the vector strength of a given unit or group and that of its

corresponding standard deviation. An equation which fits this correlation, the graph of which is shown in figure 3, with a 0.96 correlation coefficient is:

$$S = 97.3 - 18.08(L) - 67.68(L)^2$$

where,

S = Standard deviation

L = Vector strength

A group is considered here to be all the data of one particular scale of paleocurrent measurement present within a single unit. This correlation is expected because as the variability of the data increases the vector strength should decrease and the standard deviation should increase. The standard deviation is given as:

$$S^2 = \frac{\sum(\theta - \bar{\theta})^2}{(n-1)}$$

where,

S = standard deviation

$\bar{\theta}$ = vector mean

@ = datum azimuth after conversion

n = total number of data

It must be realized that because the choice of origin is critical in the determination of standard deviation, a datum azimuth must be converted to account for a new choice of origin. The vector mean was chosen as the new origin. The datum azimuth was then converted to a new azimuth such

that the numerical difference between the vector mean and that new datum azimuth would be equal to the minimum azimuthal difference between the vector mean and that datum azimuth.

VECTOR STRENGTH VS. STANDARD DEVIATION

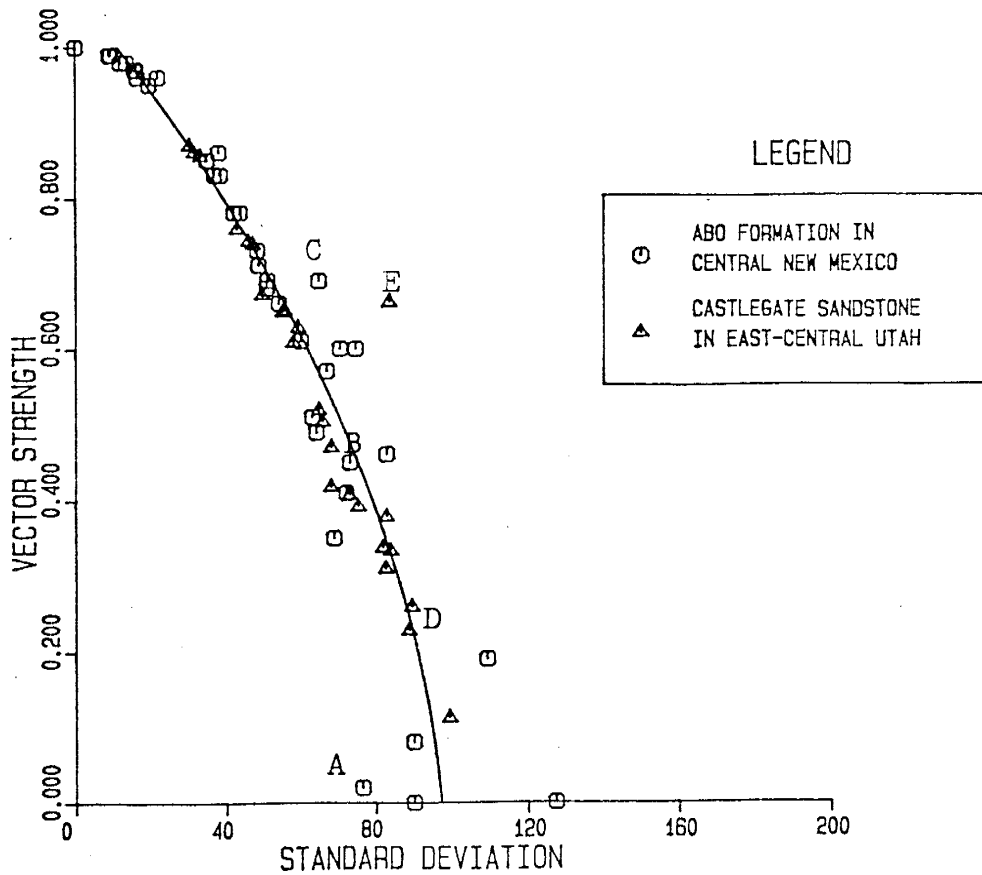


Figure 3. Vector strength vs. Standard deviation. Data for the Castlegate Sandstone taken from Van De Graaf, 1972.

Figure 3 is a plot of standard deviation verses vector strength. Figure 3 shows data collected during this study of the Abo Formation in central New Mexico and data gathered from a study of the Castlegate Sandstone of East-Central Utah (Van de Graaf, 1972). Figure 3 demonstrates that a given standard deviation may have variable and quite different vector strengths, as shown by comparison of points A,B,and C, where the standard deviation ranges from 75 to 78 but the vector strengths range from 0.02 to 0.69, and also comparison of points D and E where the standard deviation ranges from 85 to 90 but the vector strength ranges from 0.22 to 0.67. Point A is equal to lithologic unit AS122 which is bipolar (see appendix Figure F). A very low vector strength is expected for bipolar data. The maximum value for standard deviation that can be achieved for truly bipolar data approaches 127.27 degrees. This occurs with only two readings at nearly 180 degrees apart. As the number of readings increases, for bipolar data, the standard deviation approaches 90 degrees. During this time the vector strength is 0.0. The maximum difference in standard deviation that may occur for any given vector strength is thus 37.27 (127.27-90.0) degrees or 29.28% of the maximum possible value (127.27). In contrast, the maximum range in vector strength that may occur for a given standard deviation is at least 0.67 (pt.C minus pt.A) or 89.95% of the maximum value. The following conclusions are reached:

- A) The vector strength is a better indicator of the variability of directional data than is standard

deviation.

- B) A useful approximation of the true standard deviation using the equation relating vector strength (L) and standard deviation (S) previously discussed may be determined from the vector strength, but a useful approximation of the vector strength may not be determined from the standard deviation.

Tests of Significance

Different methods for determining the significance of directional data have been devised by many authors (Rayleigh, 1894; Griffiths and Rosenfeld, 1953; Gumbel et. al., 1953; Watson and Williams, 1956; Dixon and Massey, 1957; Harrison, 1957; Durand and Greenwood, 1958; Jones, 1968; Miller and Kahn, 1962). Most of these authors use standard deviation or variance along with the Student's "t" distribution, the chi square distribution and Snedecor's F distribution to infer the level of significance of directional data, assuming a circular normal population density distribution. Caution must be used in these types of analysis, as any standard deviation may have widely differing vector strengths, and thus a given standard deviation may not correctly reflect the variability of the data. If these tests are desired then the author here recommends determination of the standard deviation mathematically from the vector strength by use of the equation relating vector strength (L) and standard deviation (S). This is recommended because of the difference in range

of vector strength and standard deviation previously discussed. Another possible procedure was devised by Rayleigh (1894) which uses the quantity:

$$P = 100 - 100(e)^{-\frac{L^2}{n}(0.0001)}$$

where,

P = probability of obtaining a greater vector strength
by pure chance combination of random measurements

L = vector strength expressed in percentage

n = total number of data

The Rayleigh formula (for samples >10) tests the null hypothesis H_0 against the alternative H_a where;

H_0 = the data are randomly distributed in the interval
0 to 360 degrees

H_a = the data are not randomly distributed in the interval
0 to 360 degrees

H_0 is accepted if P is below the desired confidence level (expressed in percentage).

Durand and Greenwood (1958) suggest a modified form of the Rayleigh test for small (<10) samples. To use the Rayleigh test one must assume a circular normal distribution with prior knowledge of the possible preferred orientation and then test to see if this preferred orientation is indeed "preferred" at the desired level of significance. Prior knowledge of the preferred orientation of the paleocurrent measurement taken was not known and not enough data exist (<25) within a single unit to test for a true circular

normal distribution. Thus, the Rayleigh test was not used to compare samples of directional data in this study.

Many different methods to test the significance of directional data have been examined. Based on the results of this study, the most significant parameter appears to be the vector strength. If parametric statistics (such as mean and/or standard deviation), and/or statistical tests (using Student's "t" distribution, Snedecor's F distribution, and/or chi square distribution) are desired, then the author recommends mathematically determining standard deviation from vector strength by use of the equation relating vector strength (L) and standard deviation (S).

DEPOSITIONAL ENVIRONMENT

Introduction

The concept of uniformitarianism allows the geologist to employ recent studies of modern sedimentary depositional environments to interpret depositional environments of ancient sedimentary rocks (Allen, 1966). Using this concept, geologists agree on a fluvial and/or alluvial origin for the Abo Formation. This interpretation is based largely on stratigraphic relationships, fossil evidence and primary sedimentary structures.

Fluvial Models

Modern rivers are commonly classified into three major categories: meandering, straight, and braided. Meandering rivers are very sinuous, straight rivers are linear, and braided rivers are linear but contain intrachannel islands. This classification is somewhat arbitrary and neglects transitional patterns (Schumm, 1963). Schumm (1963) uses sinuosity (the ratio of channel length to valley length) to classify modern rivers into five major patterns, recognizing that transitional patterns exist. These patterns, as listed in increasing order of sinuosity are: straight (1.0-1.2), transitional (1.2-1.5), regular (1.5-1.75), irregular (1.75-2.0), and tortuous (>2.0). Meandering is synonymous with tortuous. Straight and braided are synonymous with straight (Schumm, 1963). The classification of Schumm (1963) is used in this study.

To study ancient fluvial environments, they must be recognized in the field. The following criteria were used

to distinguish channel sand deposits from overbank deposits in the field.

Channel Sand Deposits

- A) Dominance of medium and large scale sedimentary structures
- B) Relative absence of planar stratification structures
- C) Trough-like geometry
(lateral continuity <400 feet, 122 meters)
- D) Average grain size is usually > medium sand (0.5 mm)
- E) Poor sorting F) Thickly bedded (>1meter) or internally unstratified

Overbank Deposits

- A) Absence of medium and large scale paleocurrent indicators
- B) Abundance of stratification plane structures such as:
 - 1) Raindrop imprints
 - 2) Plant imprints
 - 3) burrows
 - 4) vertebrate tracks
- C) Tabular shaped (lateral continuity up to 800 meters, 0.5 miles)
- D) Thinly bedded
- E) Usually limited exposure due to the abundance of clay and silt

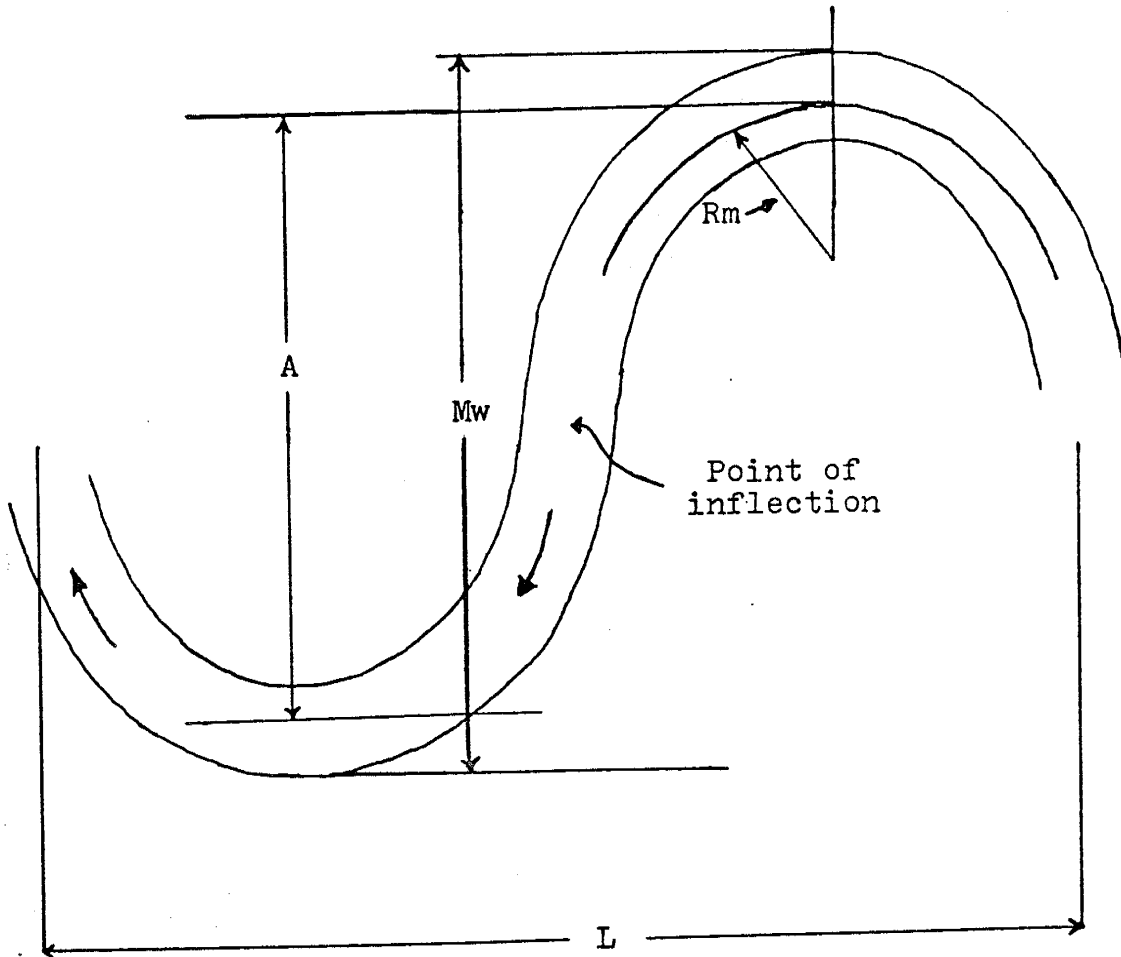
A total of four overbank deposits and nine channel sand deposits were delineated in this fashion.

Fluvial Parameters and Channel Characteristics

From the channel width, as measured perpendicular to the channel trend, and the channel depth, the following fluvial parameters may be estimated from empirically derived formulae:

- A) Channel width/ channel depth ratio
- B) Relative percentage of silt and clay and thus the bedload percentage (as later defined)
- C) Sinuosity
- D) Mean annual discharge
- E) Water velocity
- F) Water depth
- G) Froude number
- H) Meander wavelength
- I) Meander amplitude
- J) Radius of curvature
- K) Channel gradient
- L) Valley gradient
- M) Mean annual flood

A sketch which defines terms used in describing the geometric characteristics of a sinuous channel is given in Figure 4.



L = meander length (wave length)
A = amplitude
Rm = mean radius of curvature
Mw = width of meander belt

Figure 4. Sketch to define terms used in describing characteristics of a meandering channel (taken from Leopold and Wolman, 1960, figure 1)

Channel Width/ Channel Depth

The channel width/channel depth ratio (F) is primarily controlled by the type of sediment load (Schumm, 1972). As the bedload of a channel increases so does the channel width/channel depth ratio. Bedload is here defined as the material moving as surface creep plus the material moving in suspension excluding the usually small percentage of silt and clay (<0.074 mm) found in most material (Schumm, 1963 & 1972) and discussed under silt and clay percentage.

The problem of distinguishing the channel width and depth from channel-fill deposits is a major one. Unless the dimensions perpendicular to the trend of the channel can be obtained, the quantitative relationships given in Table 1 should not be used (Schumm, 1972). Criteria which help to recognize channel deposits representative of the dimensions of the channel from channel-fill deposits not representative of the dimensions of the channel are given below. Channel-fill deposits are characterized by:

- A) A channel depth greater than 20 feet, as most river channels are less than 20 feet deep (Schumm, 1972).
- B) High variability (low vector strength) of paleocurrent directions may indicate a migrating or aggrading channel
- C) The presence of two or more gravel lag deposits would probably indicate a migrating or aggrading channel.
- D) Recognition of lateral accretion beds that dip in

opposite directions.

- E) A width greater than 300 to 400 feet
(Schumm, 1972).

channel deposits are characterized by:

- A) A channel depth of up to 20 feet (Schumm, 1972).
B) A channel width up to 400 feet (Schumm, 1972).
C) Relative lack of gravel lag deposits.
D) Low variability (high vector strength) of
paleocurrent directions.

The above criteria serve only to alert the geologist to the fact that a channel-fill deposit may be present as opposed to a channel deposit, and not to distinguish one from the other.

The channel width must be measured perpendicular to the trend of the channel. Paleocurrent directions may be used to determine the trend of the channel and thus aid the geologist in determining the desired channel width.

If the empirically derived fluvial parameters thus calculated do not agree with other geologic evidence, then the geologic evidence should be considered to be of greater significance (Schumm, 1972).

Sinuosity

As can be seen in Table 1, the channel width/channel depth ratio of a channel is empirically related to the sinuosity

FLUVIAL PARAMETER	EQUATION	REFERENCE
Channel Width(cw)	-	Author
Channel Depth(cd)	-	Author
Width/Depth (F)	$F = cw/cd$	Schumm,1963
Silt and Clay % (M)	$M = 169.1(F)^{-0.926}$	Schumm,1963
Sinosity (P)	$P = 3.5(F)^{-0.25}$	Schumm,1963
Mean Annual Discharge (Qm)	$Qm = 0.056(cw)^{2.43} / F^{1.13}$	Schumm,1972
Velocity (v)*	$v = k(Qm)^m$	Leopold and Maddock,1953
Water depth (dw)*	$dw = c(Qm)^f$	Leopold and Maddock,1953
Froude Number (Fr)*	$Fr = v / [(dw)(g)]^{0.5}$	Pettijohn,Potter and Siever,1973
Meander Wavelength(ft)	$L = 18(cw)^{1.22} / cd^{0.53}$	Schumm,1972
Meander Amplitude(ft)	$A = 2.7(cw)^{1.1}$	Leopold and Wolman,1960
Radius of Curvature(ft)	$Rm = 0.206(L)^{1.02}$	Leopold and Wolman,1960
Channel Gradient(ft/mi)	$Sc = 30(F)^{0.95} / cw^{0.98}$	Schumm,1972
Valley Gradient(ft/mi)	$Cv = (Sc)(P)$	Schumm,1972
Mean Annual Flood(cfs)	$Qma = 16(cw)^{1.56} / F^{0.66}$	Schumm,1972

* k,c,m and f are empirically derived constants. As such velocity(v) and water depth(dw) were determined graphically from figures 6 and 8 of Leopold and Maddock (1953). For calculation of the Froude number, g is the constant of gravitational acceleration at the Earth's surface.

Table 1. Equations used in the calculation of various fluvial parameters

of that channel (Schumm, 1963 and 1972). As the channel width/channel depth ratio of a channel increases (increasing bedload), the sinuosity decreases. Therefore wide and shallow channels tend to be straight, whereas narrow and deep channels depart from a straight course (Schumm, 1963). As will be discussed later, the sinuosity increases with decreasing channel gradient. As a result sinuosity usually increases downstream (Schumm, 1963 and 1972; Leopold and Maddock, 1953).

Silt and Clay Percentage

The relationship between the silt and clay percentage (M) and channel width/channel depth ratio (F) is given in Table 1. An increase in the channel width/channel depth ratio is associated with a decrease in the silt and clay percentage with a subsequent increase in the bedload percentage (see Table 2). An increase in the bedload is associated with a decrease in sinuosity and a general widening of the river channel. As the percentage of cohesive materials increases (increasing percentage of silt and clay) a channel becomes more resistant to widening and thus the channel width/ channel depth ratio decreases (Schumm, 1972).

TYPE OF SEDIMENT TRANSPORT	PERCENTAGE SILT AND CLAY	PERCENTAGE BEDLOAD
SUSPENDED LOAD AND DISSOLVED LOAD	>20	<3
MIXED LOAD	5-20	3-11
BEDLOAD	<5	>11

Table 2. Sediment transport in stable alluvial channels
(taken from Schumm, 1972; table 1)

Discharge

Table 1 shows the relationship between mean annual discharge (Q_m), and the ratio of channel width (cw) to channel depth (F) (Schumm, 1972). As discharge increases so must the ratio of channel width to F . A decrease in discharge results in a decrease in bedload, and an increase in sinuosity. An increase in discharge usually results in an increase in bedload, a decrease in sinuosity, larger meander wavelengths with an associated decrease in channel gradient (Schumm, 1972). Meander wavelength and channel gradient are discussed later in this chapter. Two different rivers may have the same sinuosity but significantly different discharges. The Mississippi River from Mellwood, Arkansas to Lake Providence, Louisiana has a sinuosity of 2.1, but a mean annual discharge of 1,500,000 cubic feet per second. Whereas, Red Willow Creek in Nebraska also has a sinuosity of 2.1 but a mean annual discharge of 42 cubic feet per second (Schumm, 1963). Thus, comparison of discharge between two or more rivers should not be used to infer the sinuosity relationship between two rivers. A change in discharge in a single river will result in the changes mentioned previously.

Velocity

Water velocity (v) is largely a function of discharge (see Table 1). An increase in discharge usually results in an increase in water velocity.

Water Depth

Water depth (dw) is also largely a function of discharge (see Table 1). An increase in discharge usually results in an increase in water depth.

Froude Number

The relationship between Froude Number (Fr), water velocity (v) and water depth (dw) is shown in Table 1. The Froude Number is a dimensionless number concerned with the ratio of inertial to gravitational forces within the flow and distinguishes shooting of supercritical flow ($Fr > 1$) from tranquil or streaming or subcritical flow ($Fr < 1$) as cited by Pettijohn et. al., (1973). The Froude Number is largely a function of water velocity and to a lesser extent, water depth (dw). An increase in water velocity results in an increase in the Froude Number as well as a decrease in water depth.

Meander Wavelength

Meander wavelength is the distance along the channel axis from one point of inflection on a river to the next inflection point (see Figure 4). The relationship between meander wavelength, channel width and channel depth is given in Table 1. An increase, or very slight decrease, in the channel width/channel depth ratio causes an increase in the meander wavelength. An increase in the meander wavelength is largely a function of an increase in the channel width. As will be shown later channel width is inversely proportional to channel gradient (Schumm, 1972). Since meander wavelength and discharge are largely a function of channel width, more so than channel depth (see Table 1), an increase in discharge results in larger meander wavelengths, a decrease in sinuosity, and a decrease in channel gradient.

Meander Amplitude

Meander amplitude (A) is the distance perpendicular to the axis of a river from the center of the channel at one axis of bend to the next axis of bend (see Figure 4). As channel width increases, meander amplitude generally increases. However, meander amplitude is largely controlled by erosion characteristics of the stream banks rather than by simple hydraulic principles (Leopold and Wolman, 1960). an increase in meander amplitude indicates more erodible stream banks and should not to be used to infer hydraulic

principles. Erodibility is also dependent on vegetative growth; it is hypothesized that an increase in vegetative growth results in stabilization of the soil and thus the stream banks as well as intrachannel islands are more difficult to erode. Because of the formation of meander cut-offs, there is a general limit for the meander amplitude (Leopold and Wolman, 1960)

Mean Radius of Curvature

The relationship between mean radius of curvature (R_m) of a river bend to the meander wavelength (L) is given in Table 1. An increase in meander wavelength results in an increase in the radius of curvature. As demonstrated by Leopold and Wolman (1960), the ratio R_m/cw (mean radius of curvature/channel width) has a median value of 2.7, a mean of 3.1 with two thirds of the values (no. of values = 50) lying between 1.5 and 4.3. Thus the radius of curvature is approximately equal to three times the channel width.

Channel Gradient

The relationship between channel gradient (S_c), channel width/depth ratio (F), and channel width (cw) is given in Table 1. An increase in channel width causes a decrease in the channel gradient. Thus as the channel gradient decreases, rivers tend to get wider, but only marginally deeper. A decrease in the channel gradient is usually associated with an increase in the meander wavelength, a decrease in the bedload and an increase in the sinuosity of

the river.

Valley Gradient

The relationship between valley gradient (S_v), channel gradient (S_c), and sinuosity (P) is given in Table 1. An increase in the valley gradient is associated with an increase in the channel gradient with an associated decrease in sinuosity. Thus, as the valley gradient increases, the channel gradient must also increase at such a rate as to offset the decrease in sinuosity.

Mean Annual Flood

The relationship between mean annual flood (Q_{ma}), channel width (cw) and channel width/depth ratio (F) is given in Table 1. An increase in the mean annual flood is usually associated with a widening of the channel and subsequent decrease in the sinuosity (Schumm, 1972). If the dimensions of a channel are established primarily by flooding events, then the mean annual flood would more closely approximate the channel morphology than the mean annual discharge (Schumm, 1972).

Ephemeral flow vs. Perennial flow

The main difference between ephemeral and perennial flow appears to be discharge. Two streams, one of ephemeral flow and the other of perennial flow may have the same channel dimensions but significantly different discharges (Schumm, 1972). The equation in Table 1 would yield a much

higher estimate of the mean annual discharge than is appropriate for ephemeral stream channels. Ephemeral streams are usually associated with a dry climate. Schumm (1972) recommends that if evidence exist that a particular channel is associated with a dry climate, then the mean annual discharge calculated from the equation in Table 1 should be reduced by one-half. Hunt (1983) determined by examination of plant fauna present within the Abo Formation near the study area that, a semi-arid climate with episodes of dryness existed for the Abo Formation during Late Wolfcampian and Leonardian time.

Paleocurrent Analysis

The Lower Arkose unit of the Abo Formation yielded only one channel sand deposit (AMS25) with sufficient exposure to permit the collection of paleocurrent data. The Middle Mudstone Unit was too poorly exposed to permit the collection of paleocurrent data. Seven channel sand deposits and four overbank deposits were identified within the Upper Sandstone Unit of the Abo formation (see Figure 3).

Rose diagrams along with the paleocurrent data for each lithologic unit are given in the Appendix (Figures A-M, Tables A-M). Table 3 gives the resulting paleocurrent statistics for each unit. The units studied are given here in ascending stratigraphic order. The determination of channel sand deposits and overbank deposits was done in the

field using the criteria previously mentioned.

Lower Arkose Unit

Analysis of lithologic unit AMS25 (Table 3, appendix, Figure A) yields a channel sand deposit with a westerly paleocurrent direction. Paleocurrent directions for medium and large scale paleocurrent structures differ by 42 degrees. There are many different explanations for this difference. One explanation is that large scale paleocurrent structures may represent lateral accretion beds (Allen, 1966) and thus an angular difference of 42 degrees is entirely possible. Another possible explanation is that in any fluvial system, there are many different types of currents which are oblique to the main current. All these currents contribute to the variability of the paleocurrent directions as measured from primary sedimentary structures. At any rate a westerly-northwesterly direction is indicated for this lithologic unit.

Middle Mudstone Unit

The Middle Mudstone Unit occurs within the study area. However, the quality of exposure was sufficiently poor as to prohibit the collection of paleocurrent data.

LITHOLOGIC UNIT (INTERPRETATION)	TYPE	VECTOR STRENGTH	VECTOR MEAN	STANDARD DEVIATION	N	RANKING	PALEOCURRENT DIRECTION
AS412 (OVERBANK)	S	0.51	270.24	63.20	13	-	
	M	-	-	-	0	-	
	L	-	-	-	0	-	
	ALL	0.51	270.24	63.20	13		
AS410 (OVERBANK)	S	0.73	190.28	48.56	12	B	
	M	0.86	127.67	38.20	3	A	
	L	-	-	-	0	-	
	ALL	0.68	177.37	51.01	15		
AS47 (CHANNEL SAND)	S	0.57	225.77	67.03	18	B	
	M	0.78	324.87	43.85	5	A	
	L	-	-	-	0	-	
	ALL	0.45	247.58	73.22	23		
AS45 (CHANNEL SAND)	S	-	-	-	1	-	
	M	0.35	48.79	68.96	13	-	
	L	-	-	-	1	-	
	ALL	0.41	38.90	72.26	15		
AS38 (CHANNEL SAND)	S	0.60	293.74	70.61	5	B	
	M	0.83	266.73	37.03	7	A	
	L	0.60	188.62	74.79	10	B	
	ALL	0.49	242.03	64.28	22		
AMS215 (OVERBANK)	S	0.08	45.53	89.98	15	-	
	M	-	-	-	0	-	
	L	-	-	-	0	-	
	ALL	0.08	45.53	89.98	15		
AS122 BIPOLAR, (OVERBANK)	S	0.02	50.06	76.48	14	-	
	M	-	-	-	0	-	
	L	-	-	-	0	-	
	ALL	0.02	50.06	76.48	14		
AS119C (CHANNEL SAND)	S	0.78	240.03	42.32	13	B	
	M	0.98	249.36	13.67	7	A	
	L	-	-	-	0	-	
	ALL	0.85	243.77	35.04	20		
AS119A (CHANNEL SAND)	S	0.46	191.58	82.94	3	C	
	M	0.66	293.18	54.28	7	B	
	L	0.99	285.16	9.47	4	A	
	ALL	0.61	280.63	60.18	14		
AS119B (CHANNEL SAND)	S	0.99	227.00	9.00	3	A	
	M	0.98	196.18	12.03	5	B	
	L	0.69	144.00	65.05	2	C	
	ALL	0.83	199.12	38.62	10		
AMS211 (CHANNEL SAND)	S	0.97	274.41	15.71	11	A	
	M	0.95	263.26	19.60	5	B	
	L	0.97	272.96	16.27	8	A	
	ALL	0.96	271.62	16.58	24		
AMS25 (CHANNEL SAND)	S	-	-	-	1	-	
	M	0.69	315.76	51.31	15	B	
	L	0.96	273.43	21.92	2	A	
	ALL	0.71	307.80	48.95	18		

INTERPRETATION	AVERAGE VECTOR STRENGTH			ALL
	SMALL	MEDIUM	LARGE	
CHANNEL SAND	0.73	0.77	0.84	0.61
OVERBANK	0.46	0.86*	--	0.32
COMBINED	0.61	0.79	--	0.52

* only one occurrence

Table 3. Statistics as calculated from the equations given in the text. Lithologic units are listed upward in ascending stratigraphic order. In terms of vector strength, A = highest ranked, B = second, and C = third.

Upper Sandstone UnitPaleocurrent Directions

The lowest lithologic unit in the Upper sandstone unit is AMS211. Examination of Table 3 and the rose diagram (Appendix, Figure B) yields a channel sand deposit with a strong westerly paleocurrent direction. All paleocurrent structures agree with this direction. Thus a westerly paleocurrent direction is indicated for this channel sand deposit.

The next higher lithologic unit is AS119B (see photo 1). Examination of Table 3 and the rose diagram (Appendix, Figure C) yields a channel sand deposit with a south-southwesterly paleocurrent direction. All measured paleocurrent structures agree with this direction with small scale paleocurrent structures varying by only 30 degrees westward. One large paleocurrent structure indicates an easterly current, this is believed by the author to represent a lateral accretion bed. Thus the strike of this bed should approximate the paleocurrent direction of the channel (Allen, 1966). A paleocurrent direction of south-southwesterly agrees with this interpretation. Thus a paleocurrent direction of south-southwesterly is indicated for this channel sand deposit.

The next higher lithologic unit is AS119A (see photos 1 & 2). Examination of Table 3 and the rose diagram (Appendix, Figure D) yields a channel sand deposit with a

west-northwestly paleocurrent direction. Medium and large scale paleocurrent structures agree with a west-northwesterly paleocurrent direction. Small scale paleocurrent structures indicate a direction that is approximately 90 degrees farther to the south. This is believed by the author to be the result of cross currents or eddy currents. Thus a west-northwesterly paleocurrent direction is indicated for this channel sand deposit.

The next higher lithologic unit is AS119C (see photo 2). Examination of Table 3 and the rose diagram (Appendix, Figure E) yields a channel sand deposit with a west-southwesterly paleocurrent direction. There are no large scale paleocurrent structures. Medium and small scale paleocurrent structures both agree well with a west-southwesterly paleocurrent direction for this channel sand deposit.

Lithologic unit AS122 is laterally continuous with AS119C. Examination of Table 3 and the rose diagram (Appendix, Figure F) indicates lithologic unit AS122 is an overbank deposit with a bipolar (northwest-southeast) paleocurrent direction. As will be shown in a later chapter, overbank deposits should not be used to determine paleocurrent directions.

The next higher lithologic unit is AMS215. Examination of Table 3 and the rose diagram (Appendix, Figure G) yields an overbank deposit with an extremely variable paleocurrent direction. As will be discussed later, paleocurrent directions from overbank deposits should not be used.

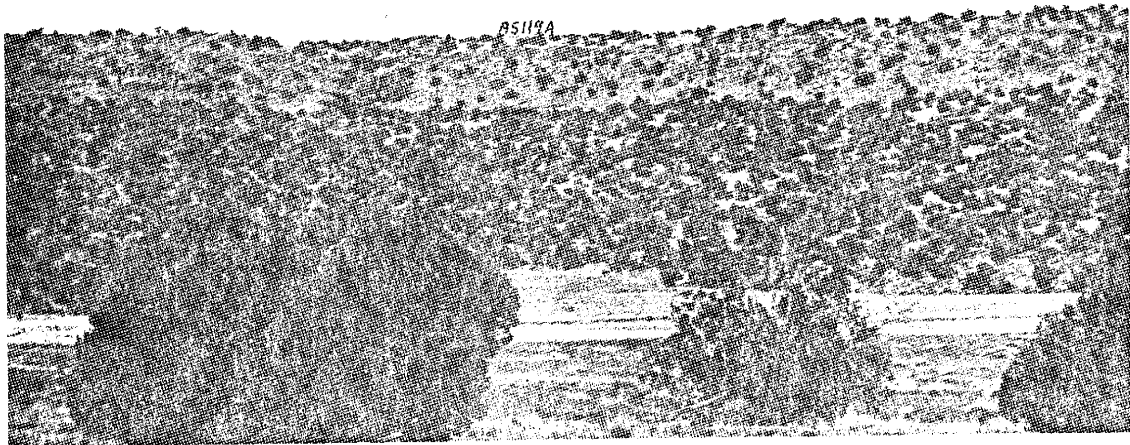


Photo 1. View looking west of lithologic units AS119A and AS119B.

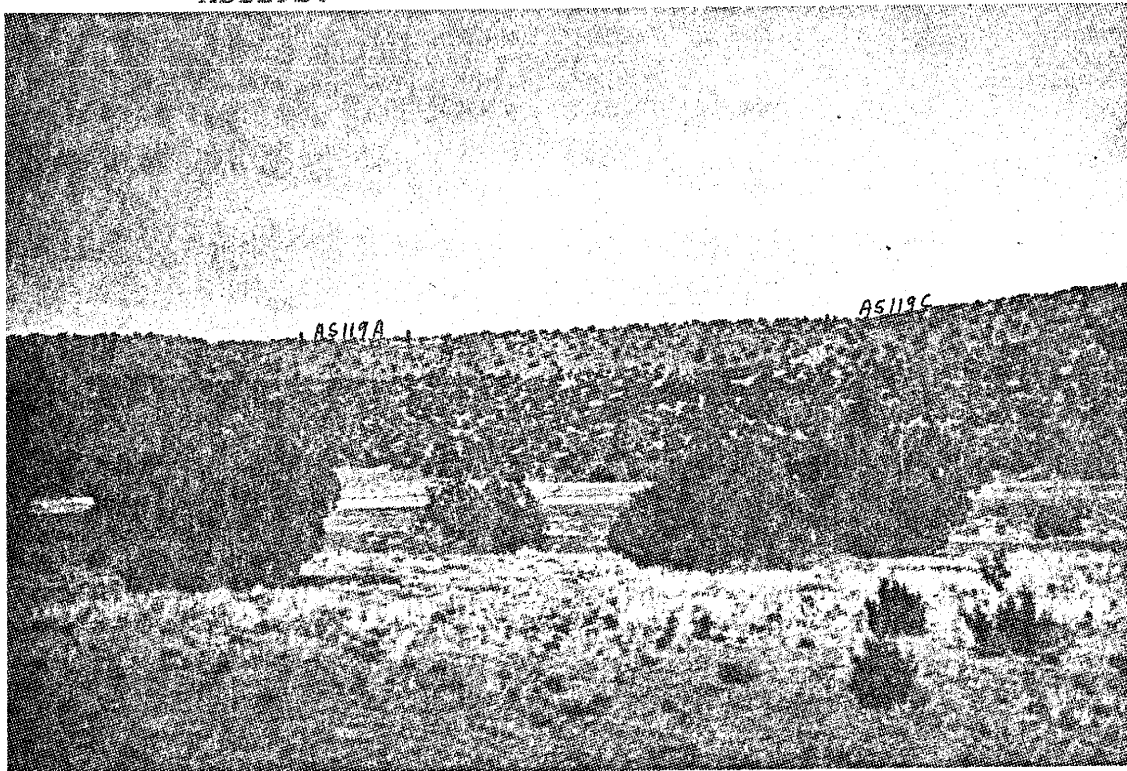


Photo 2. View looking west of lithologic units AS119A and AS119C.

The next higher lithologic unit is AS38. Examination of Table 3 and the rose diagram (Appendix, Figure H) yields a channel sand deposit with a westerly paleocurrent direction. Large scale paleocurrent structures indicate southerly and northerly paleocurrent directions. These are believed by the author to be lateral accretion beds and as such the strike of these beds should approximate the paleocurrent direction (Allen, 1966). As such, a westerly paleocurrent direction is indicated because small and medium scale paleocurrent structures indicate a westerly paleocurrent direction for this channel sand deposit.

The next higher lithologic unit is AS45. Examination of Table 3 and the rose diagram (Appendix, Figure I) yields a channel sand deposit with a highly variable but northeasterly paleocurrent direction. The variability of paleocurrent directions may be explained by examination of Table 4. A tortuous river channel is indicated for the lithologic unit stratigraphically above and an irregular river channel for the lithologic unit stratigraphically below. These lithologic units have relatively small meander wavelengths. Thus, if one were to measure paleocurrent directions along a bend in a meander, varying paleocurrent directions would be measured. This is what has probably happened here. A northeasterly paleocurrent direction is tentatively interpreted for this lithologic unit. However, not much credence is given to this interpretation because of the highly variable paleocurrent direction.

The next higher lithologic unit is AS47. Examination

of Table 3 and the rose diagram (Appendix, Figure J) yields a channel sand deposit with a highly variable but northwesterly paleocurrent direction. Small scale paleocurrent structures indicate a wide range in paleocurrent directions. This is believed to be caused by eddy currents and cross currents. Medium scale paleocurrent structures indicate a much more confined range in paleocurrent directions. This would indicate that in this instance, medium scale paleocurrent structures were less affected by eddy and cross currents. Thus, medium scale paleocurrent structures would more closely approximate the paleocurrent direction of the channel. As a result a northwesterly paleocurrent direction is interpreted for this channel sand deposit.

The next higher lithologic unit is AS410. Examination of Table 3 and the rose diagram (Appendix, Figure K) yields as overbank deposit with a southerly paleocurrent direction. As will be discussed later paleocurrent directions from overbank deposits should not be used to interpret the paleocurrent direction of the adjacent river channel.

The next higher lithologic unit is AS412. Examination of Table 3 and the rose diagram (Appendix, Figure L) indicates an overbank deposit with a bimodal (north-northwesterly and southwesterly) paleocurrent pattern. As will be discussed later, paleocurrent directions from overbank deposits should not be used to interpret the paleocurrent direction of the river channel.

Fluvial Parameter Analysis

Table 4 gives the results of five lithologic units for which channel width and depth determinations were made. All these lithologic units are present within the Upper Sandstone Unit of the Abo Formation (see Figure 3). The lithologic units in Table 4 are listed from left to right in descending stratigraphic order.

As we move in ascending stratigraphic (see Table 4 and Figure 5) order from lithologic unit AS119B to AS119A to AS119C the following are observed:

- A) An increase in bedload
- B) A decrease in sinuosity
- C) An increase followed by a stabilization in the mean annual discharge
- D) An increase in meander wavelength
- E) An increase in meander amplitude
- F) An increase in the radius of curvature
- G) A decrease followed by a gentle increase in both the channel gradient and valley gradient
- H) An increase followed by a stabilization of the mean annual flood

(47)

LITHOLOGIC UNIT	AS47	AS38	AS119C	AS119A	AS119B
WIDTH(ft)	150	160	<1300	1000	275
DEPTH(ft)	20	15	20	30	20
WIDTH/DEPTH	7.5	10.67	<65	33.3	13.75
VECTOR STRENGTH	0.45	0.49	0.85	0.61	0.83
SILT AND CLAY %	26.2	18.9	>3.54	6.6	14.93
% BEDLOAD	<3	4	>11	9	6
SINOUSITY	2.03	1.85	>1.13	1.36	1.72
SINOUSITY TERM	TORTUOUS	IRREGULAR	STRAIGHT	TRANSITIONAL	REGULAR
MEAN ANNUAL DISCHARGE(cfs)	1106	869	<18,323	20,623	2432
VELOCITY(ft/s)	2.3	1.9	<2.9	3.0	2.4
WATER DEPTH(ft)	2.5	2.1	<7.5	7.7	3.5
FROUDE NUMBER	0.26	0.23	>0.19	0.19	0.23
FROUDE TERM	TRANQUIL	TRANQUIL	TRANQUIL	TRANQUIL	TRANQUIL
MEANDER WAVELENGTH(ft)	1662	2094	<23,160	13,564	3,481
MEANDER AMPLITUDE(ft)	668	718	<7,189	5,387	1,302
RADIUS OF CURVATURE(ft)	397	503	<5833	3380	844
CHANNEL GRADIENT(ft/mi)	1.50	1.97	>1.40	0.96	1.47
VALLEY GRADIENT(ft/mi)	3.04	3.64	>1.58	1.30	2.53
MEAN ANNUAL FLOOD(cfs)	10,502	9,203	<73,341	75,736	18,121

Note: units are listed from left to right in descending stratigraphic order

Table 4. Fluvial parameter results as calculated from the equations given in table 1.

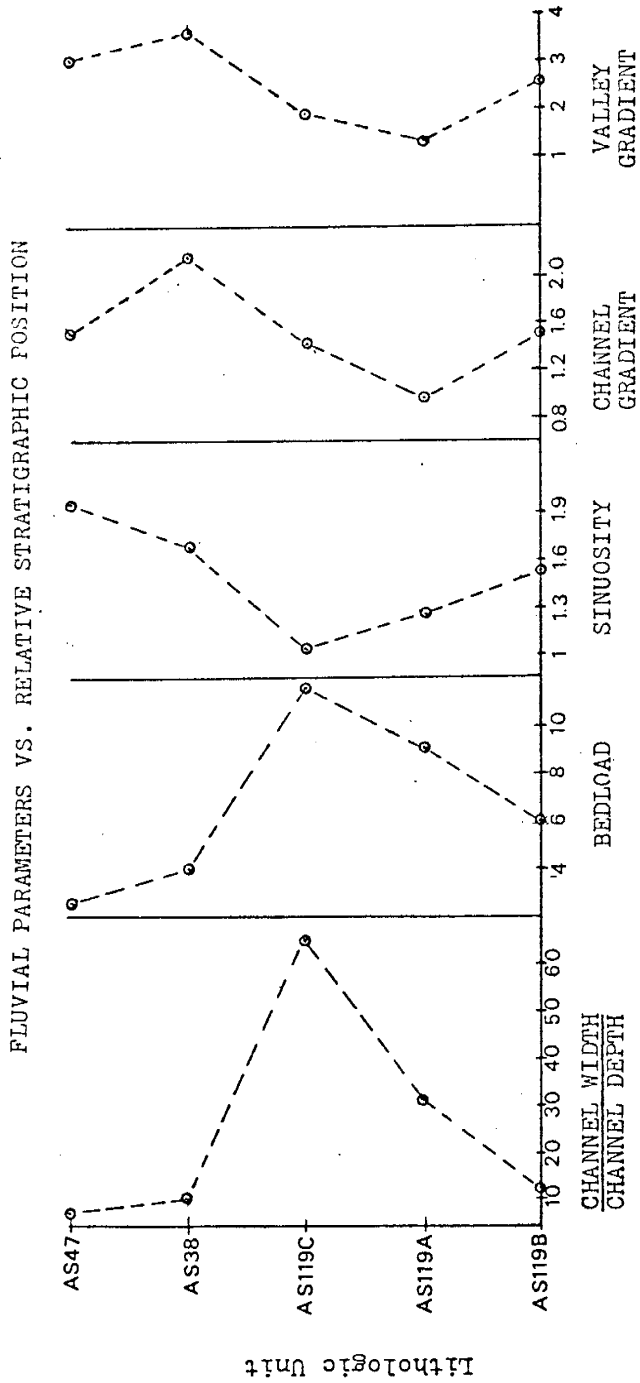


Figure 5. The vertical axis is not to scale. Bedload is given in percentage (%), channel and valley gradients are in ft/mi.

An increase in sinuosity will, by use of the equations in Table 1, mathematically result in increases in the mean annual discharge, meander wavelength, meander amplitude, the radius of curvature, and in the mean annual flood. Thus changes in bedload, sinuosity, channel gradient, and valley gradient are used to infer changes in the depositional environment.

An increase in bedload is most probably associated with an increase in relief between the source area and the study area. As the bedload increases the sinuosity decreases (see Figure 5). The decrease in channel and valley gradients observed is most likely a result of an increase in base level. An increase in relief between the source area and the study area is usually associated with an increase in valley gradient with a subsequent increase in channel gradient. This is what is observed between lithologic units AS119A and AS119C. However, between lithologic units AS119B and AS119A the opposite is true. This is believed to reflect a rise in base level and thus a subsequent decrease in channel gradient with a resulting mathematical decrease in valley gradient. Thus, from lithologic units AS119B to AS119A an increase in base level resulted in a decrease in channel and valley gradients. An increase in relief between the source area and the study area accompanied by an associated increase in bedload, resulted in a decrease in sinuosity. The increase in discharge is most probably associated with an increase in runoff.

Continuing in ascending stratigraphic order, lithologic

units AS119C, AS38 and AS47 are encountered. Comparison of these lithologic units in Table 4 and Figure 5 yields the following observations:

- A) A decrease in bedload
- B) A dramatic increase in the sinuosity
- C) A decrease followed by a stabilization in the mean annual discharge
- D) A dramatic decrease in the meander wavelength
- E) A decrease in the meander amplitude
- F) A dramatic decrease in the radius of curvature
- G) An increase followed by a decrease in both the channel and valley gradients
- H) A decrease followed by a stabilization of the mean annual flood

The decrease in bedload is most probably the result of a decrease in relief between the source area and the study area, retreating source area, or progressively finer sediment being eroded from the source area. The increase in channel and valley gradients from lithologic units AS119C to AS38 most probably reflects basin subsidence of the study area at such a rate as to offset the decrease in bedload. The decrease in channel and valley gradients from lithologic units AS38 to AS47 most probably reflects a rise in base level and/or filling of the channel.

Not only do we observe a gentle rise followed by a gentle decrease in both the channel and valley gradients, but also that the channel gradient is approximately one-half that of the valley gradient. An explanation is given

by Schumm (1963). As base level begins to rise the channel gradient is decreased and thus the coarser sediment is deposited (see lithologic units AS119B and AS119A). As base level continues to rise progressively finer sediments are deposited, as in lithologic units AS119C, AS38 and AS47, until finally the river is only transporting the finest fraction of its previous load. Thus the load of a river is changing from coarser material to finer material throughout time. As a result, rivers draining areas of mixed sediments, after deposition of the coarser fraction, were flowing on alluvium with a gradient in excess of that required for transport of the finer fraction. A reduction of the gradient by degradation could only partly reduce the stream gradient, because with incision the river encounters the coarser sediments which serve as an armor and thus prevent further degradation. As a result the channel gradient could not increase.

Regional Depositional System

The upper sandstone unit of the Abo Formation is characterized by a general increase in the relief between the study area and the source area up through lithologic unit AS119C and then a decrease in relief between the study area and the source area and/or a retreating source area up through deposition of lithologic unit AS47. A rise in base level is believed to have occurred throughout this time. This rise in base level may be associated with a rise in sea level. However, the proximity of the shoreline to the Abo

Formation at the study area during Wolfcampian -Leonardian time is not known. Thus a rise in sea level may or may not have been "felt" by the fluvial system of the Abo Formation. Paleocurrent directions indicate a dominantly westward flowing system.

Kottowski and Stewart (1970) believed that the Pedernal landmass was covered or partially covered by the clastic debris of the Abo Formation by Late Wolfcampian time. This observation agrees with either an apparent decrease in relief between the study area and the source area or a retreating source area. This change in relief or retreating edge of the source area is believed to occur between lithologic units AS119C and AS38. If we accept the time sequence given by Kottowski and Stewart (1970) during which the Abo Formation began to cover the Pedernal landmass, the Wolfcampian - Leonardian time boundary might occur somewhere between lithologic unit AS119C and the overlying Yeso Formation. However, not enough data is present in this study to substantiate this hypothesis.

STATATISTICAL COMPARISON OF SCALED PALEOCURRENT STRUCTURES

Introduction

Flume studies indicate that primary sedimentary structures created from a fluvial current are good indicators of the direction of the current at that precise location. However, in most fluvial environments, many flow regimes exist at the same time, but at different locations, and thus many smaller currents exist, such as eddy, cross, etc., that are oblique to the main current. Another observation that follows is that smaller currents (smaller mean flow velocity/mean flow depth ratio) can only create smaller scale primary sedimentary structures. Thus smaller scale paleocurrent indicators would be more variable than larger scale paleocurrent indicators. Geologists are usually concerned with the direction of the main current as this is used to infer the paleoslope dip direction. As a result, some geologists believe that large scale primary sedimentary structures are the best indicators of the paleoslope dip direction. This direction is herein referred to as the "true" paleocurrent direction.

Small vs. Medium vs. Large Scale Paleocurrent Indicators
Within a Single Unit and Between Units of Similar
Paleoenvironment

Small Scale

Small scale paleocurrent indicators are present within overbank deposits as well as channel sands. Only those present within channel sands will be discussed in this section of the study.

Ranking of paleocurrent measurements, determined from primary sedimentary structures of different scales is based on comparison of their vector strengths as shown in Table 3. Thus in unit AS119A, large scale paleocurrents have a vector strength of 0.99 and is ranked highest or A, medium scale paleocurrents have a vector strength of 0.66 and is ranked second or B, and small scale paleocurrents have a vector strength of 0.46 and is ranked third or C. In terms of vector strength, Table 3 shows that small scale paleocurrent measurements rank first in two instances, second in four instances, and in third two instances. The average vector strength is 0.73 and ranges from 0.46 to 0.97 in lithologic units AS119A and AMS211 respectively.

Medium Scale

Medium scale paleocurrent indicators are almost solely confined to channel sands. The only occurrence within an overbank deposit is in lithologic unit AS410.

In terms of vector strength, Table 3 shows that medium scale paleocurrent measurements rank first in four instances, second in four instances, and never third. The average vector strength is 0.77 and ranges from 0.35 to 0.98 for lithologic units AS45 and AS119B and/or AS119C respectively.

Large Scale

Large scale paleocurrent indicators are restricted solely to channel sand lithologic units.

In terms of vector strength, Table 3 shows that large scale paleocurrent measurements rank first in three instances, second in one instance, and third in one instance. There are only two data present in which the ranking of third was achieved (see lithologic unit AS119B). The average vector strength is 0.84 and ranges from 0.60 to 0.99 in lithologic units AS38 and AS119A respectively.

Conclusions

Based upon the average vector strength, the range of vector strengths previously discussed and the relative ranking of the different scales of paleocurrent measurements taken within a single lithologic unit and between lithologic units of similar paleoenvironment, the following conclusions are reached:

- A) Large scale paleocurrent indicators are the least variable, both within a single lithologic unit and between lithologic units of similar paleoenvironment

- B) Medium scale paleocurrent indicators are slightly more variable than large scale paleocurrent indicators, but less variable than small scale paleocurrent indicators. This variability exists both within a single lithologic unit and between lithologic units of similar paleoenvironment.
- C) Small scale paleocurrent indicators are the most variable of all the paleocurrent indicators studied. This variability exists both within a single lithologic unit and between lithologic units of similar paleoenvironment.
- D) Not enough difference exists between the average vector strengths as determined for small, medium and large scale paleocurrent indicators, either within a single lithologic unit or between lithologic units of similar paleoenvironment, to warrant "weighting" the particular paleocurrent measurement taken for use in statistical analysis.

Channel Sand Deposits vs. Overbank Deposits

As shown in Table 3, the average vector strength for channel sand deposits is 0.61. In contrast, the average vector strength for overbank deposits is 0.32. Assuming a linear relationship in vector strengths, overbank deposits are twice as variable as channel sand deposits. Small scale paleocurrent indicators are about 1.5 times as variable in overbank deposits as they are in channel sand deposits. Only one occurrence (AS410) exists where medium scale

paleocurrent indicators occur within an overbank deposit. For this reason, the author believes that data are insufficient to properly evaluate the variability of medium scale paleocurrent indicators between overbank deposits and channel sand deposits.

Comparison of a Channel Sand Deposit and It's Adjacent Overbank Deposit

Lithologic unit AS122, which is an overbank deposit, rests conformably upon lithologic unit AS119A, and is laterally continuous with lithologic unit AS119C. Lithologic unit AS122 is bipolar (see rose diagram appendix, Figure F) in nature with one mode at N 30 W and the other mode at S 45 E. Lithologic unit AS119C has a vector mean of S 64 W, which is approximately at right angles to either mode present in lithologic unit AS122.

Lithologic unit AS119A has a vector mean of N 80 W (see Table 3 and the rose diagram in the appendix, Figure D) The minimum azimuthal difference between the vector means of lithologic units AS119A and AS122 is 50 degrees.

Overbank deposits which occur stratigraphically between channel sand deposits appear to be unrelated in terms of direction to the subjacent and superjacent channel sand deposits. This difference is evident between lithologic units AS119C, AS122 and AMS21, also between lithologic units AMS21, AMS215 and AS38 and finally between lithologic units AS47 and AS410.

All these data indicate that overbank deposits may not

be used to infer the "true" paleocurrent direction of the laterally continuous or adjacent channel sand deposit, or channel sand deposits that may occur either stratigraphically above or below the particular overbank deposit in question. Moreover, if paleocurrent data from overbank deposits are combined with paleocurrent data from laterally continuous channel sand deposits, as done by Cappa and MacMillan (1983), it would only decrease the vector strength, alter the resultant vector direction (vector mean) and increase the range and variability of data about the vector mean. Therefore it is not recommended that paleocurrent measurements from channel sand deposits and those from overbank deposits be combined for analysis.

APPENDIX

Note:

Type 1 = small scale paleocurrent structures

Type 2 = medium scale paleocurrent structures

Type 3 = large scale paleocurrent structures

→ S = vector mean direction for small scale
paleocurrent structures

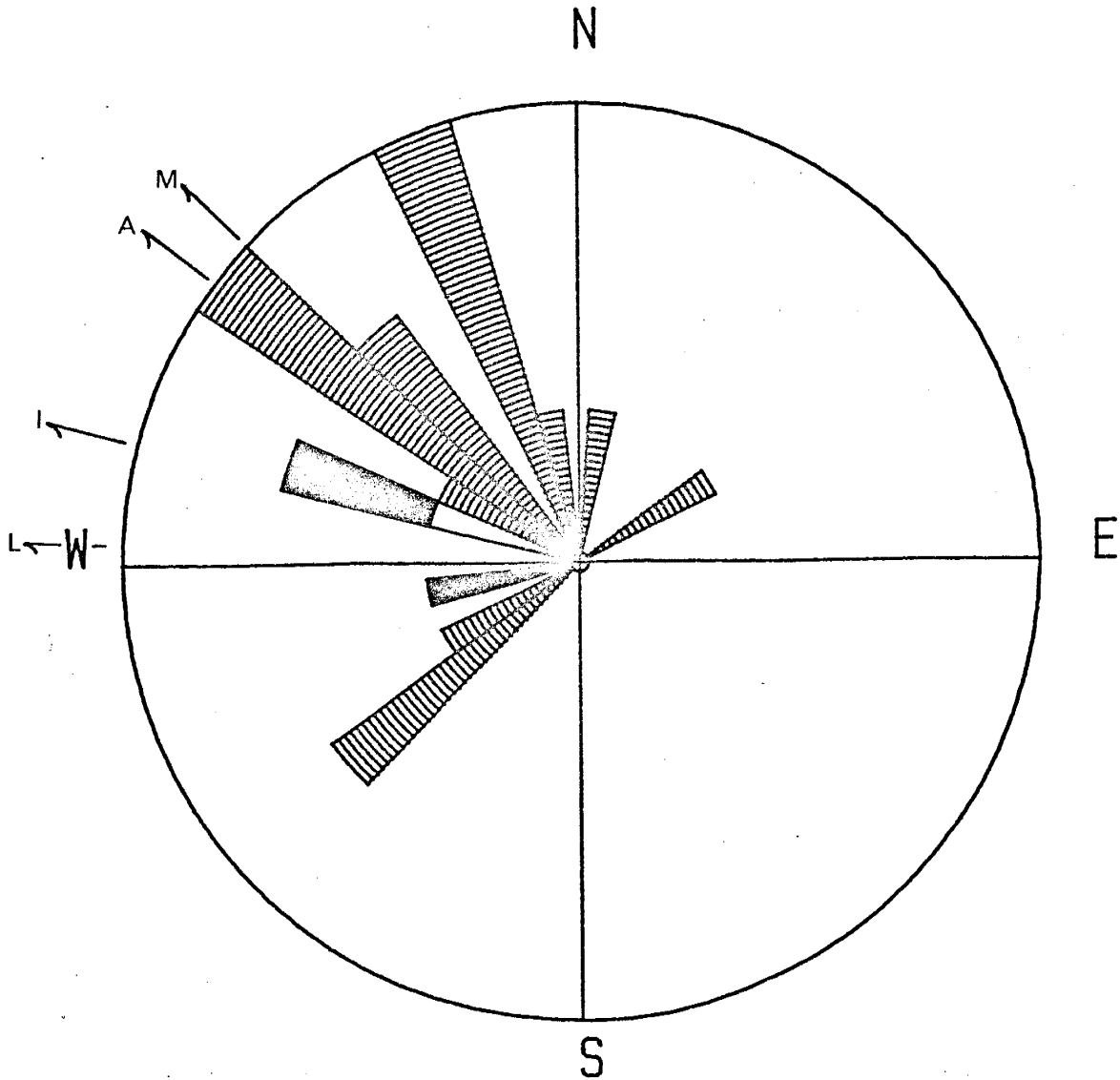
→ M = vector mean direction for medium scale
paleocurrent structures

→ L = vector mean direction for large scale
paleocurrent structures

→ A = combined total vector mean direction

→ I = interpreted paleocurrent direction

CHANNEL SAND



LEGEND



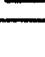
DATAFILE =	AMS25
NO. MEASUREMENTS =	18
VECTOR MEAN =	307.8
VECTOR STRENGTH =	0.71
RADIUS =	3 MEASUREMENTS
	LARGE SCALE PALEOCURRENTS
	MEDIUM SCALE PALEOCURRENTS
	SMALL SCALE PALEOCURRENTS

Figure A

DATAFILE = AMS25
 ORIGINAL AND ROTATED DATA

	DIRECTION		ORIGINAL DATA		TYPE	CORRECTED AZIMUTH
			AZIMUTH	INCLINATION		
REGIONAL:	S	55 E	125	4		
CURRENT BEDDING:	S	88 W	268	3	3	289
	S	75 E	105	5	2	57
	N	45 W	315	15	2	313
	N	35 W	325	13	2	320
	N	70 W	290	5	2	297
	N	10 W	350	12	2	339
	N	60 E	60	2	2	335
	S	35 W	215	15	2	230
	S	33 W	213	15	2	228
	N	40 W	320	23	2	318
	N	85 W	275	5	1	288
	N	35 E	35	10	2	13
	N	15 W	345	15	2	337
	N	5 E	5	12	2	351
	N	45 W	315	5	2	311
	N	55 W	305	5	2	305
	S	3 E	177	3	3	258
	S	55 W	235	20	2	244

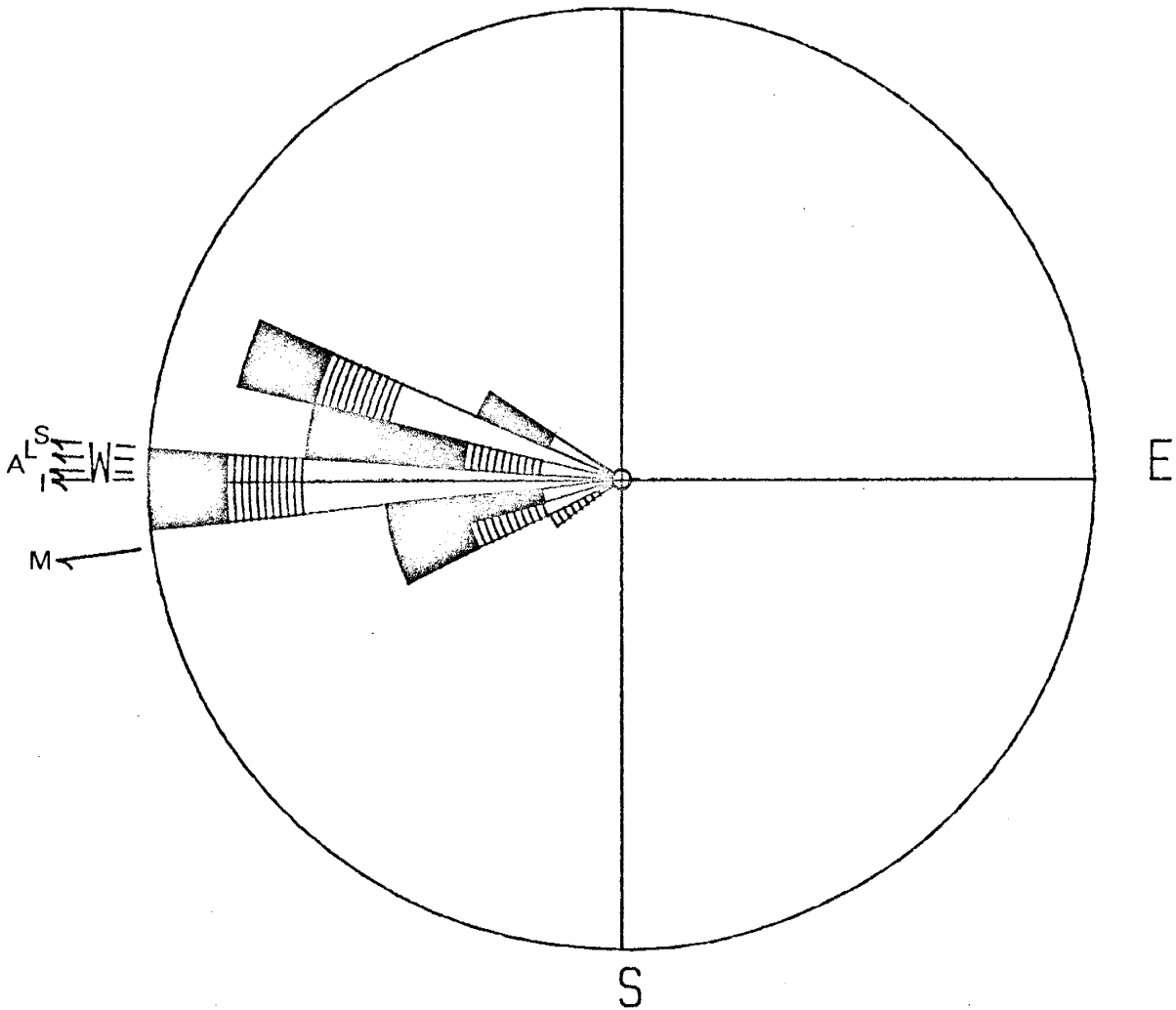
STATISTICAL SUMMARY:
 NUMBER OF VALUES: 18
 VECTOR MEAN: 307.84
 RESULTANT: 12.72
 VECTOR STRENGTH: 0.71

FREQUENCY TABULATION	
SECTOR	FREQUENCY
5- 14	1
15- 24	0
25- 34	0
35- 44	0
45- 54	0
55- 64	1
65- 74	0
75- 84	0
85- 94	0
95-104	0
105-114	0
115-124	0
125-134	0
135-144	0
145-154	0
155-164	0
165-174	0
175-184	0
185-194	0
195-204	0
205-214	0
215-224	0
225-234	2
235-244	1
245-254	0
255-264	1
265-274	0
275-284	0
285-294	2
295-304	1
305-314	3
315-324	2
325-334	0
335-344	3
345-354	1
355- 4	0

Table A.

CHANNEL SAND

N



LEGEND




DATAFILE =	AMS211
NO. MEASUREMENTS =	24
VECTOR MEAN =	271.6
VECTOR STRENGTH =	0.96
RADIUS =	6 MEASUREMENTS
	LARGE SCALE PALEOCURRENTS
	MEDIUM SCALE PALEOCURRENTS
	SMALL SCALE PALEOCURRENTS

Figure B.

DATAFILE = AMS211
 ORIGINAL AND ROTATED DATA

	DIRECTION	ORIGINAL DATA		TYPE	CORRECTED AZIMUTH
		AZIMUTH	INCLINATION		
REGIONAL:	S 75 E	105	15		
CURRENT BEDDING:	S 65 E	115	5	1	280
	S 40 E	140	10	1	245
	S 15 W	195	15	2	239
	N 10 W	350	5	1	300
	S 25 W	205	5	1	268
	N 75 W	285	8	3	285
	S 20 W	200	10	3	252
	S 25 W	205	5	2	268
	S 85 W	265	7	3	278
	N 50 W	310	0	1	285
	S 45 W	225	12	3	258
	N 45 W	315	20	3	303
	S 0 W	180	10	2	247
	N 50 W	310	5	1	291
	N 70 W	290	10	1	287
	S 70 W	250	5	3	276
	S 70 W	250	15	1	267
	S 70 W	250	15	1	267
	S 30 W	210	5	1	268
	S 45 W	225	10	1	261
	N 20 W	340	0	2	285
	S 65 W	245	9	3	270
	S 50 W	230	10	3	263
	S 80 W	260	7	2	277

FREQUENCY TABULATION

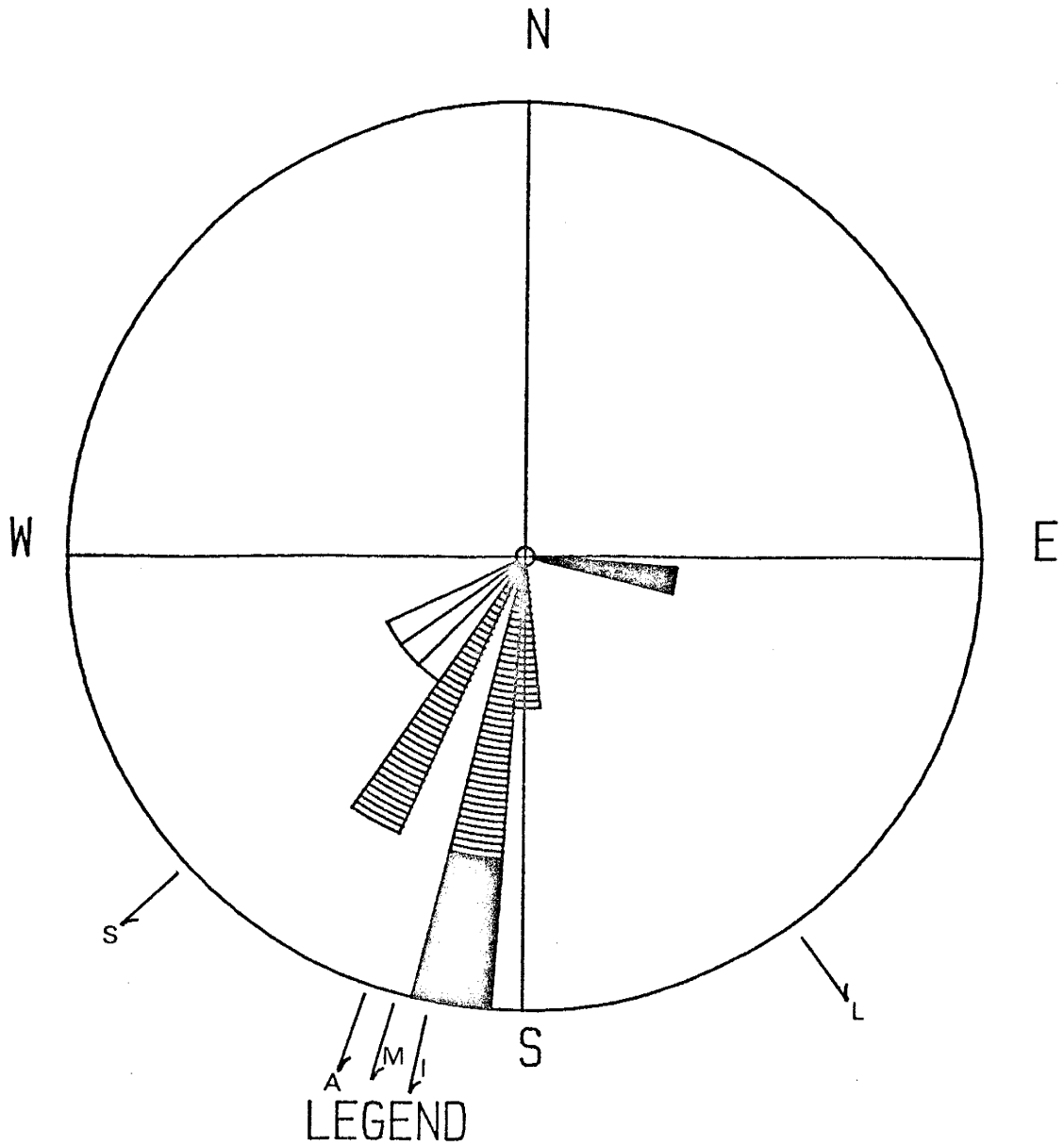
SECTOR	FREQUENCY
5- 14	0
15- 24	0
25- 34	0
35- 44	0
45- 54	0
55- 64	0
65- 74	0
75- 84	0
85- 94	0
95-104	0
105-114	0
115-124	0
125-134	0
135-144	0
145-154	0
155-164	0
165-174	0
175-184	0
185-194	0
195-204	0
205-214	0
215-224	0
225-234	0
235-244	1
245-254	3
255-264	3
265-274	6
275-284	4
285-294	5
295-304	2
305-314	0
315-324	0
325-334	0
335-344	0
345-354	0
355- 4	0

STATISTICAL SUMMARY:

NUMBER OF VALUES: 24
 VECTOR MEAN: 271.65
 RESULTANT: 23.05
 VECTOR STRENGTH: 0.96

Table B.

CHANNEL SAND



LEGEND



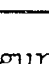
DATAFILE =	AS119B
NO. MEASUREMENTS =	10
VECTOR MEAN =	199.2
VECTOR STRENGTH =	0.83
RADIUS =	3 MEASUREMENTS
	LARGE SCALE PALEOCURRENTS
	MEDIUM SCALE PALEOCURRENTS
	SMALL SCALE PALEOCURRENTS

Figure C.

LITHOLOGIC UNIT = AS119B
 ORIGINAL AND ROTATED DATA

	DIRECTION	ORIGINAL DATA		TYPE	CORRECTED AZIMUTH
		AZIMUTH	INCLINATION		
REGIONAL:	S 75 E	105	4		
CURRENT BEDDING:	S 45 W	225	15	1	236
	S 10 W	190	10	2	212
	S 80 E	100	15	3	98
	S 10 E	170	10	2	193
	S 15 E	165	10	2	188
	S 10 E	170	5	1	218
	S 5 W	185	5	1	227
	S 10 W	190	15	2	205
	S 20 E	160	10	2	183
	S 5 E	175	15	3	190

STATISTICAL SUMMARY:

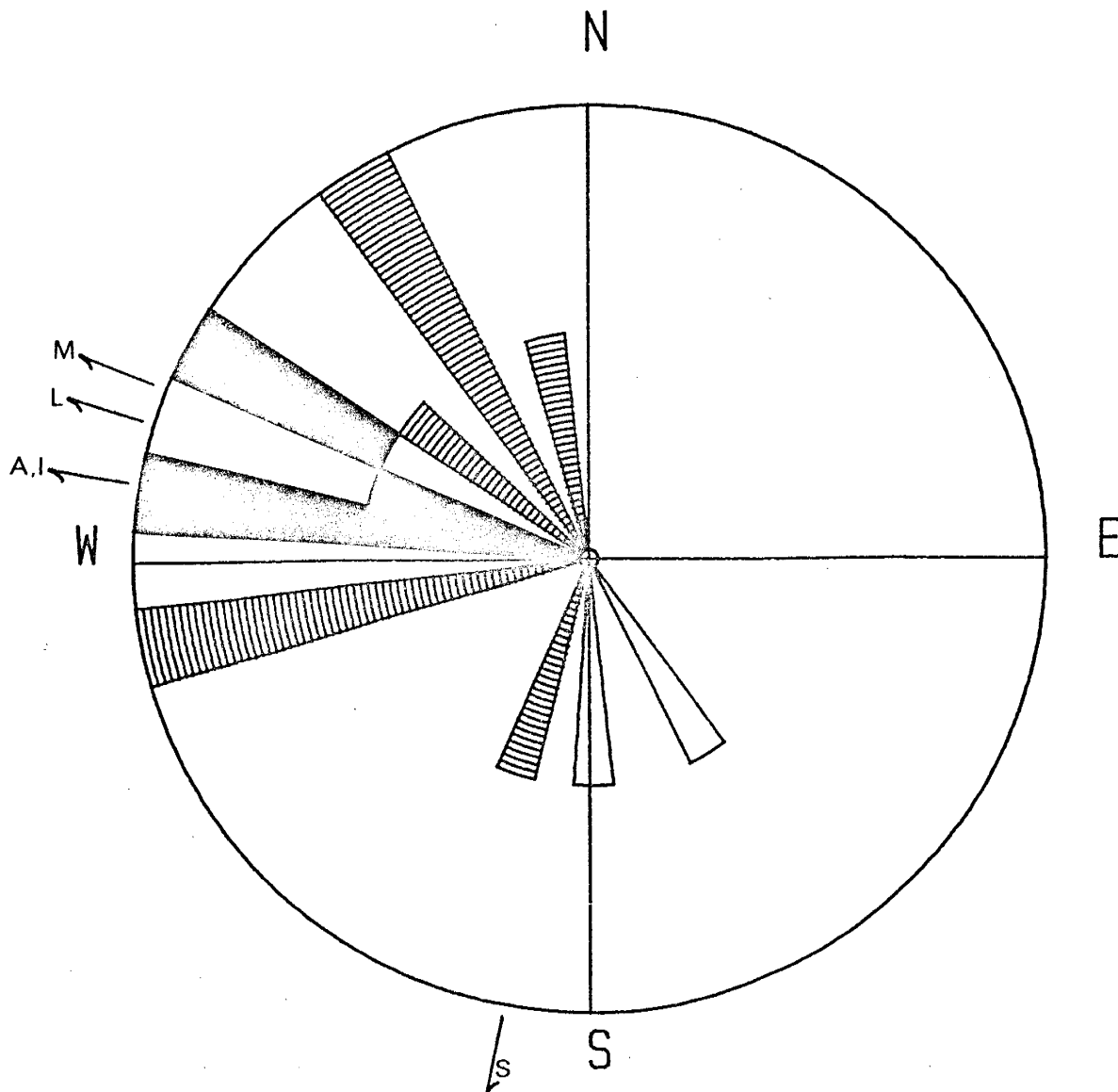
NUMBER OF VALUES: 10
 VECTOR MEAN: 199.25
 RESULTANT: 8.33
 VECTOR STRENGTH: 0.83

FREQUENCY TABULATION

SECTOR	FREQUENCY
5- 14	0
15- 24	0
25- 34	0
35- 44	0
45- 54	0
55- 64	0
65- 74	0
75- 84	0
85- 94	0
95-104	1
105-114	0
115-124	0
125-134	0
135-144	0
145-154	0
155-164	0
165-174	0
175-184	1
185-194	3
195-204	0
205-214	2
215-224	1
225-234	1
235-244	1
245-254	0
255-264	0
265-274	0
275-284	0
285-294	0
295-304	0
305-314	0
315-324	0
325-334	0
335-344	0
345-354	0
355- 4	0

Table C.

CHANNEL SAND



LEGEND




DATAFILE =	AS119A
NO. MEASUREMENTS =	14
VECTOR MEAN =	280.6
VECTOR STRENGTH =	0.61
RADIUS =	2 MEASUREMENTS
	LARGE SCALE PALEOCURRENTS
	MEDIUM SCALE PALEOCURRENTS
	SMALL SCALE PALEOCURRENTS

Figure D.

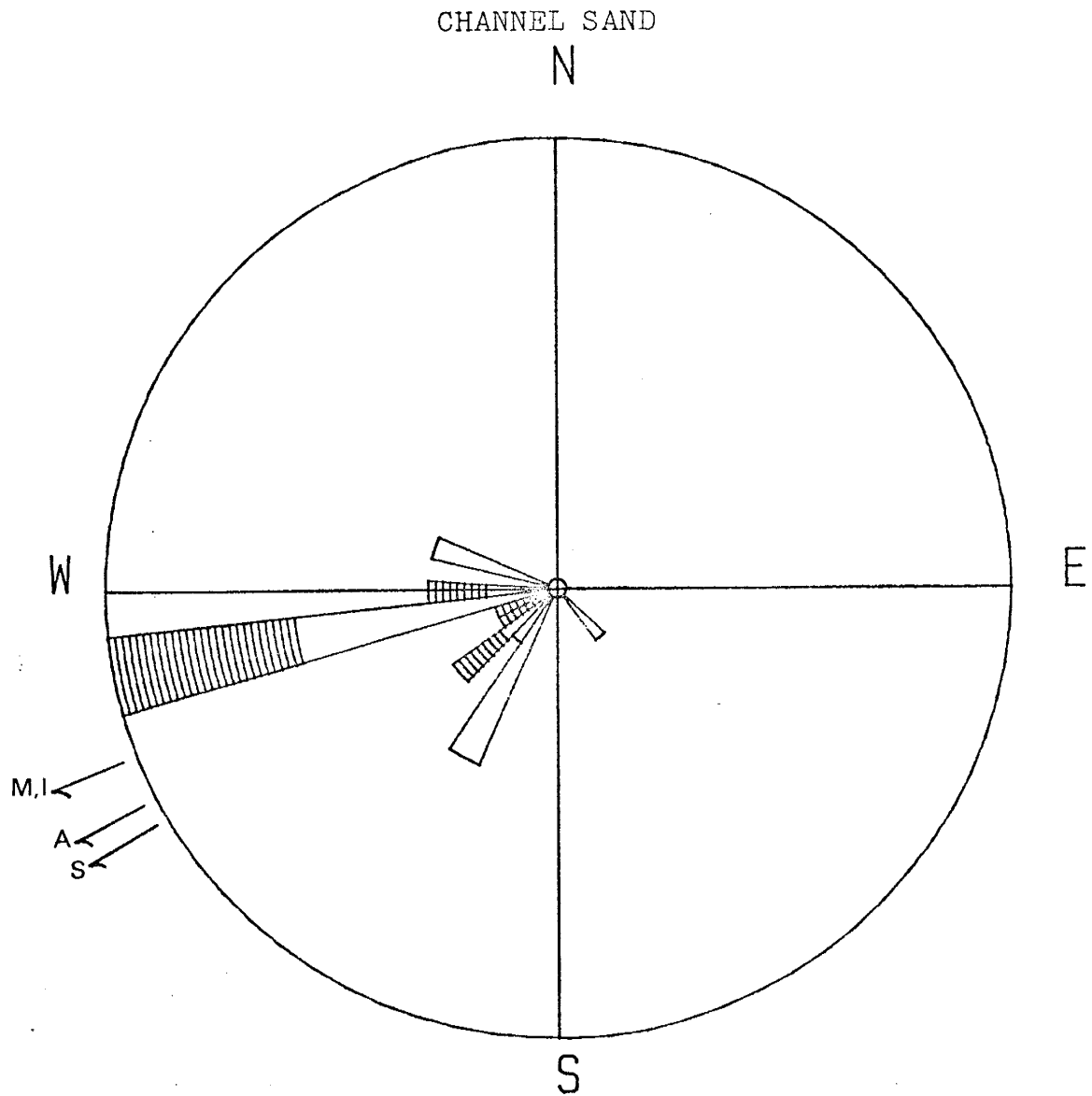
LITHOLOGIC UNIT = AS119A
 ORIGINAL AND ROTATED DATA

	DIRECTION	ORIGINAL DATA		TYPE	CORRECTED AZIMUTH
		AZIMUTH	INCLINATION		
REGIONAL:	N 90 E	90	0		
CURRENT BEDDING:	S 75 W	255	5	2	255
	N 60 W	300	15	3	300
	N 30 W	330	15	2	330
	N 75 W	285	10	3	285
	N 10 W	350	10	2	350
	S 30 E	150	10	1	150
	N 60 W	300	5	1	300
	N 80 W	280	20	3	280
	N 55 W	305	10	2	305
	N 30 W	330	10	2	330
	N 80 W	280	15	3	280
	S 75 W	255	10	2	255
	S 20 W	200	20	2	200
	S 5 E	175	5	1	175

STATISTICAL SUMMARY:
 NUMBER OF VALUES: 14
 VECTOR MEAN: 280.63
 RESULTANT: 8.50
 VECTOR STRENGTH: 0.61

FREQUENCY TABULATION	
SECTOR	FREQUENCY
5- 14	0
15- 24	0
25- 34	0
35- 44	0
45- 54	0
55- 64	0
65- 74	0
75- 84	0
85- 94	0
95-104	0
105-114	0
115-124	0
125-134	0
135-144	0
145-154	1
155-164	0
165-174	0
175-184	1
185-194	0
195-204	1
205-214	0
215-224	0
225-234	0
235-244	0
245-254	0
255-264	2
265-274	0
275-284	2
285-294	1
295-304	2
305-314	1
315-324	0
325-334	2
335-344	0
345-354	1
355- 4	0

Table D.



LEGEND

DATAFILE =	AS119C
NO. MEASUREMENTS =	20
VECTOR MEAN =	243.8
VECTOR STRENGTH =	0.85
RADIUS =	7 MEASUREMENTS
LARGE SCALE PALEOCURRENTS	
MEDIUM SCALE PALEOCURRENTS	
SMALL SCALE PALEOCURRENTS	

Figure E.

LITHOLOGIC UNIT = AS119C
ORIGINAL DATA

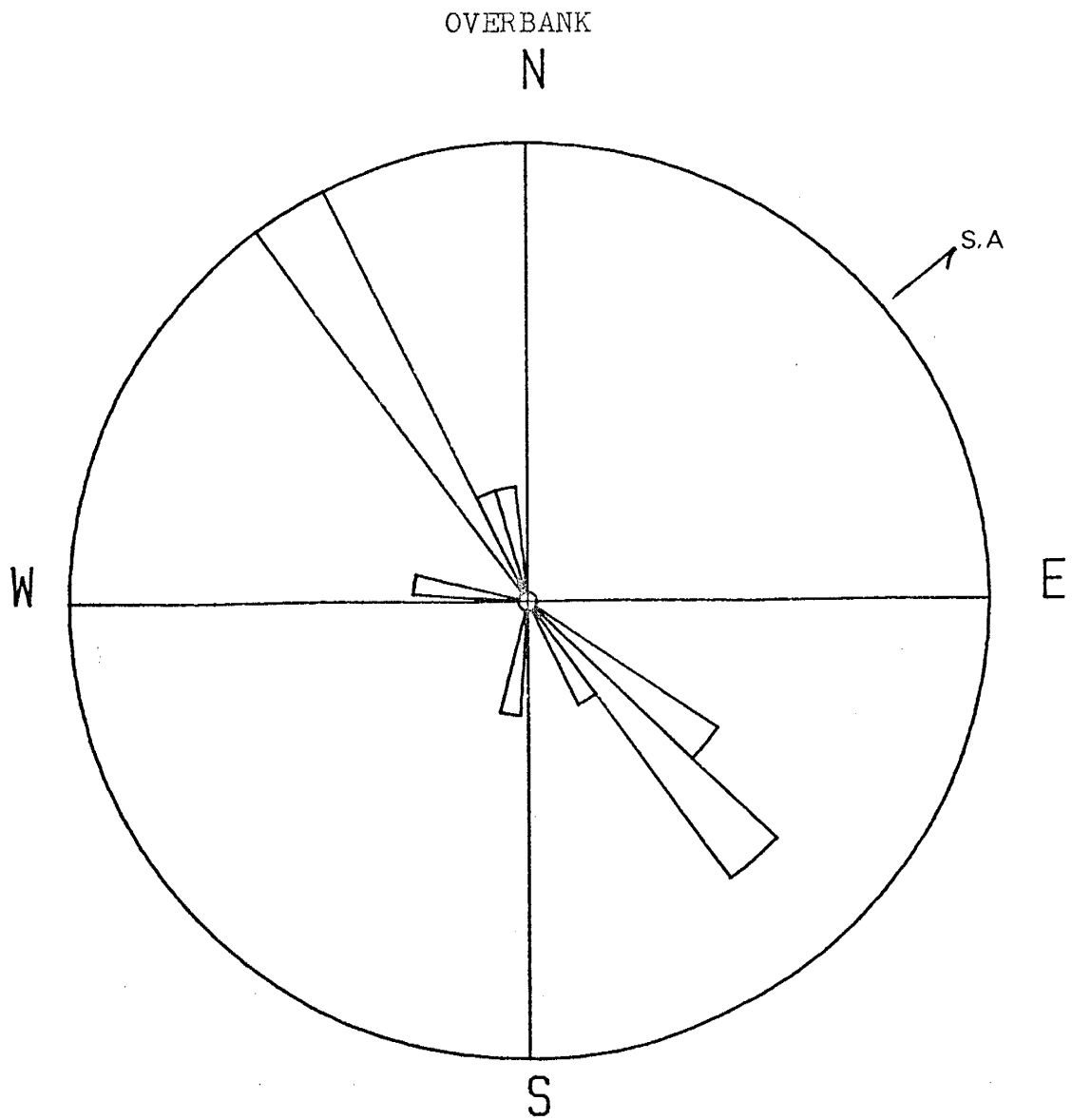
DIRECTION	AZIMUTH	INCLINATION	TYPE
S 45 E	135	0	1
S 48 W	228	15	1
S 30 W	210	5	1
S 75 W	255	20	2
S 75 W	255	5	1
S 30 W	210	5	1
S 45 W	225	10	2
S 80 W	260	5	1
N 75 W	285	5	1
N 70 W	290	5	1
S 80 W	260	10	2
S 35 W	215	5	1
S 25 W	205	5	1
S 75 W	255	10	2
S 85 W	265	10	2
N 90 W	270	5	1
S 80 W	260	5	1
S 75 W	255	0	1
S 65 W	245	5	2
S 60 W	240	10	2

STATISTICAL SUMMARY:
NUMBER OF VALUES: 20
VECTOR MEAN: 243.77
RESULTANT: 16.98
VECTOR STRENGTH: 0.85

FREQUENCY TABULATION

SECTOR	FREQUENCY
5- 14	0
15- 24	0
25- 34	0
35- 44	0
45- 54	0
55- 64	0
65- 74	0
75- 84	0
85- 94	0
95-104	0
105-114	0
115-124	0
125-134	0
135-144	1
145-154	0
155-164	0
165-174	0
175-184	0
185-194	0
195-204	0
205-214	3
215-224	1
225-234	2
235-244	1
245-254	1
255-264	7
265-274	2
275-284	0
285-294	2
295-304	0
305-314	0
315-324	0
325-334	0
335-344	0
345-354	0
355- 4	0

Table E.



LEGEND

DATAFILE =	AS122
NO. MEASUREMENTS =	14
VECTOR MEAN =	50.1
VECTOR STRENGTH =	0.02
RADIUS =	4 MEASUREMENTS
LARGE SCALE PALEOCURRENTS	
MEDIUM SCALE PALEOCURRENTS	
SMALL SCALE PALEOCURRENTS	

Figure F.

LITHOLOGIC UNIT = AS122

ORIGINAL DATA			
DIRECTION	AZIMUTH	INCLINATION	TYPE
S 10 W	190	0	1
N 30 W	330	0	1
S 45 E	135	0	1
S 50 E	130	0	1
N 80 W	280	0	1
S 30 E	150	0	1
N 30 W	330	0	1
S 40 E	140	0	1
N 35 W	325	0	1
S 50 E	130	0	1
N 25 W	335	0	1
S 45 E	135	0	1
N 30 W	330	0	1
N 15 W	345	0	1

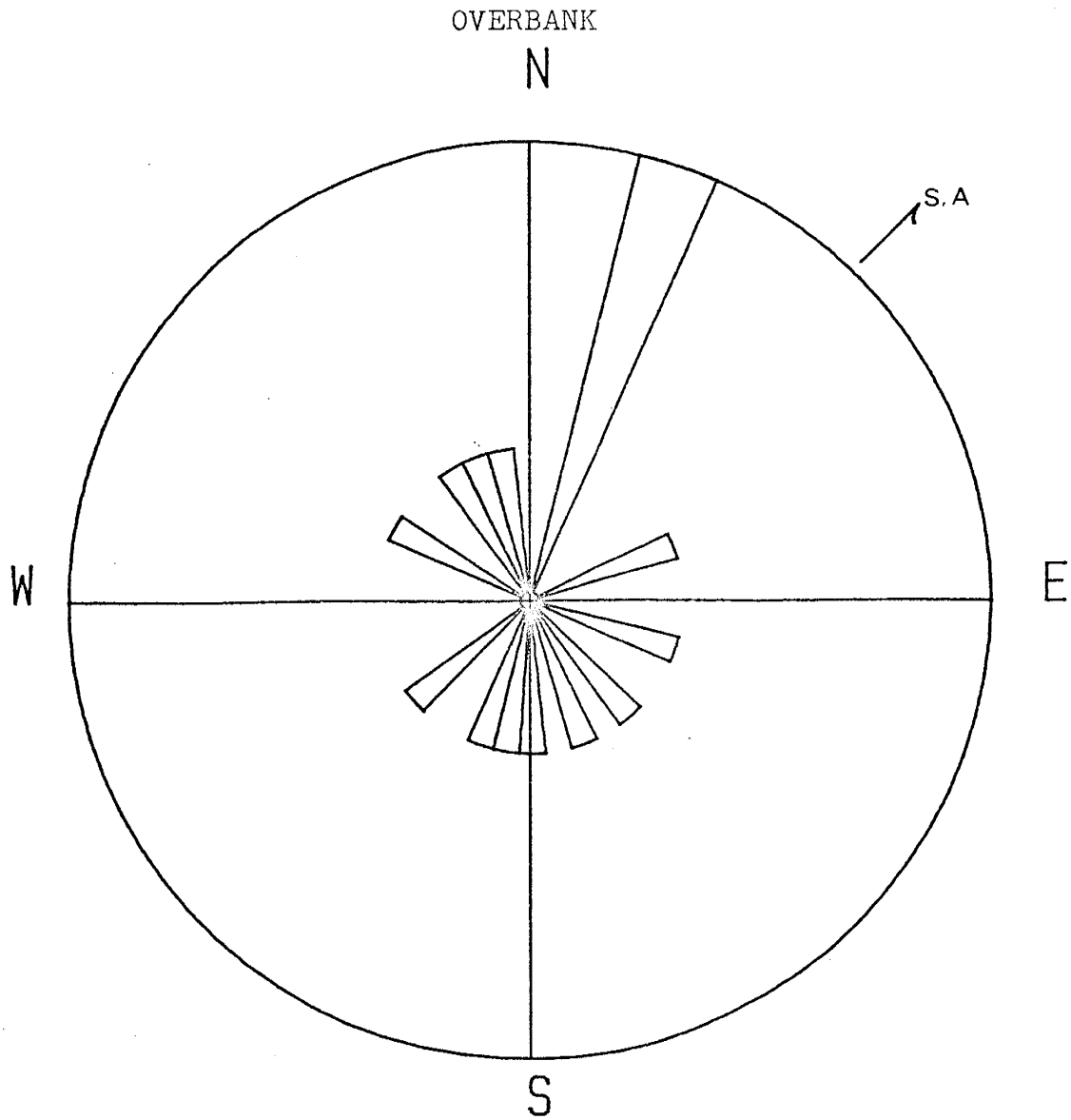
STATISTICAL SUMMARY:

NUMBER OF VALUES: 14
 VECTOR MEAN: 50.06
 RESULTANT: 0.22
 VECTOR STRENGTH: 0.02

FREQUENCY TABULATION

SECTOR	FREQUENCY
5- 14	0
15- 24	0
25- 34	0
35- 44	0
45- 54	0
55- 64	0
65- 74	0
75- 84	0
85- 94	0
95-104	0
105-114	0
115-124	0
125-134	2
135-144	3
145-154	1
155-164	0
165-174	0
175-184	0
185-194	1
195-204	0
205-214	0
215-224	0
225-234	0
235-244	0
245-254	0
255-264	0
265-274	0
275-284	1
285-294	0
295-304	0
305-314	0
315-324	0
325-334	4
335-344	1
345-354	1
355- 4	0

Table F.



LEGEND

DATAFILE =	AMS215
NO. MEASUREMENTS =	15
VECTOR MEAN =	44.5
VECTOR STRENGTH =	0.08
RADIUS =	3 MEASUREMENTS
LARGE SCALE PALEOCURRENTS	
MEDIUM SCALE PALEOCURRENTS	
SMALL SCALE PALEOCURRENTS	

Figure G.

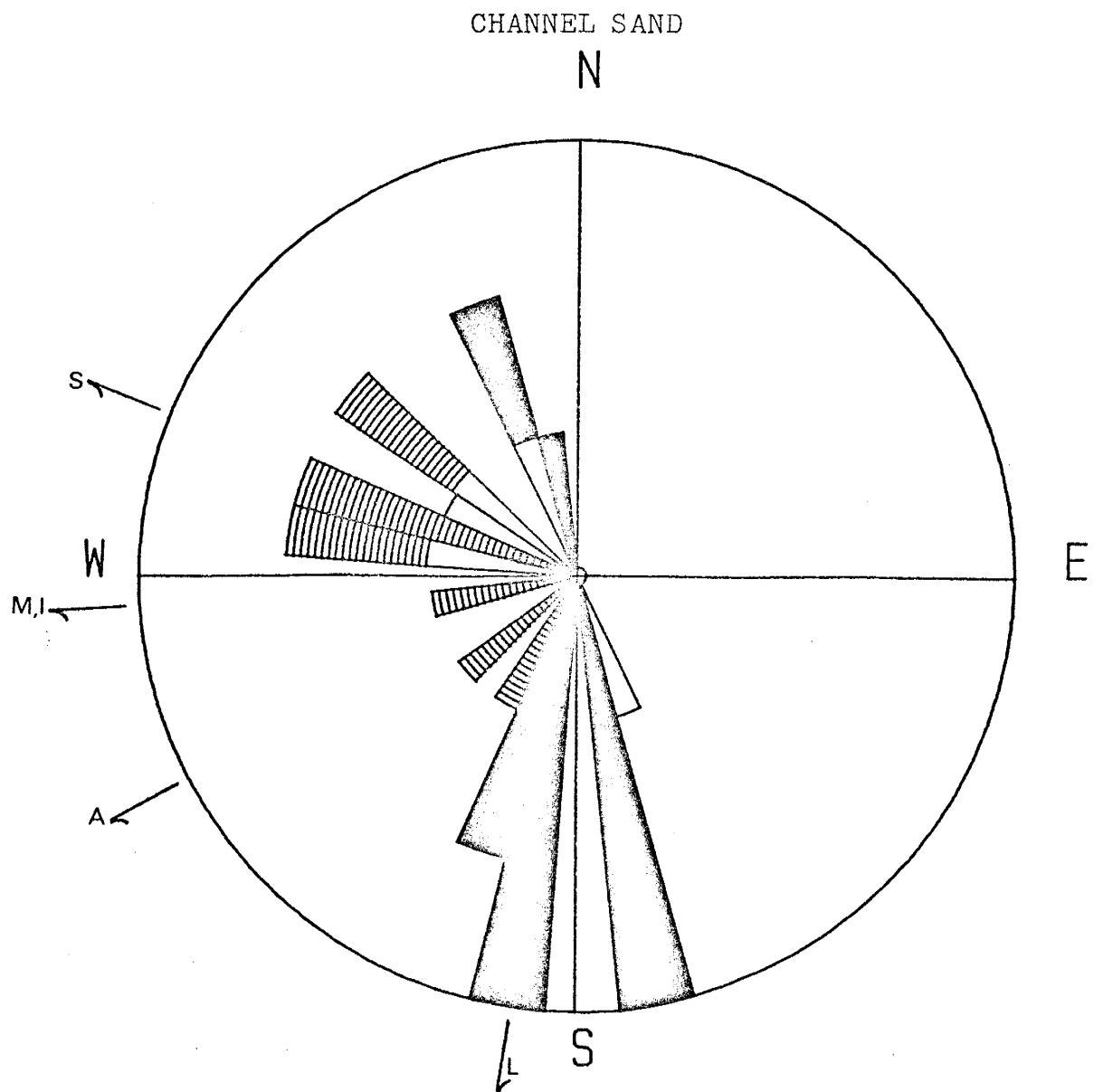
LITHOLOGIC UNIT = AMS215
 ORIGINAL AND ROTATED DATA

	DIRECTION	ORIGINAL DATA		TYPE	CORRECTED AZIMUTH
		AZIMUTH	INCLINATION		
REGIONAL:	N 75 W	285	3		
CURRENT BEDDING:	S 50 W	230	5	1	193
	S 40 W	220	3	1	162
	S 45 W	225	8	1	203
	N 40 W	320	10	1	333
	N 60 W	300	3	1	24
	N 70 W	290	5	1	297
	N 50 W	310	5	1	339
	N 60 W	300	3	1	24
	S 30 W	210	5	1	175
	S 80 W	260	2	1	140
	S 80 W	260	5	1	231
	N 55 W	305	4	1	346
	N 65 E	65	15	1	71
	N 75 W	285	3	1	105
	N 60 W	300	3	1	24

STATISTICAL SUMMARY:
 NUMBER OF VALUES: 15
 VECTOR MEAN: 44.47
 RESULTANT: 1.16
 VECTOR STRENGTH: 0.08

FREQUENCY TABULATION	
SECTOR	FREQUENCY
5- 14	0
15- 24	3
25- 34	0
35- 44	0
45- 54	0
55- 64	0
65- 74	1
75- 84	0
85- 94	0
95-104	0
105-114	1
115-124	0
125-134	0
135-144	1
145-154	0
155-164	1
165-174	0
175-184	1
185-194	1
195-204	1
205-214	0
215-224	0
225-234	1
235-244	0
245-254	0
255-264	0
265-274	0
275-284	0
285-294	0
295-304	1
305-314	0
315-324	0
325-334	1
335-344	1
345-354	1
355- 4	0

Table G.



LEGEND

DATAFILE =	AS38
NO. MEASUREMENTS =	22
VECTOR MEAN =	242.0
VECTOR STRENGTH =	0.49
RADIUS =	3 MEASUREMENTS
LARGE SCALE PALEOCURRENTS	
MEDIUM SCALE PALEOCURRENTS	
SMALL SCALE PALEOCURRENTS	

Figure H.

LITHOLOGIC UNIT = AS38

ORIGINAL DATA				
DIRECTION		AZIMUTH	INCLINATION	TYPE
N	80 W	280	10	1
S	9 E	171	22	3
S	15 W	195	18	3
S	5 W	185	25	3
S	20 W	200	15	3
S	5 W	185	23	3
N	70 W	290	10	2
N	50 W	310	10	2
N	10 W	350	15	3
N	20 W	340	21	3
N	25 W	335	0	1
S	15 E	165	10	3
S	20 E	160	12	1
S	30 W	210	8	2
S	45 W	225	15	2
S	10 W	190	12	3
S	9 E	171	25	3
N	55 W	305	0	1
N	60 W	300	0	1
N	70 W	290	10	2
N	80 W	280	15	2
S	75 W	255	8	2

STATISTICAL SUMMARY:

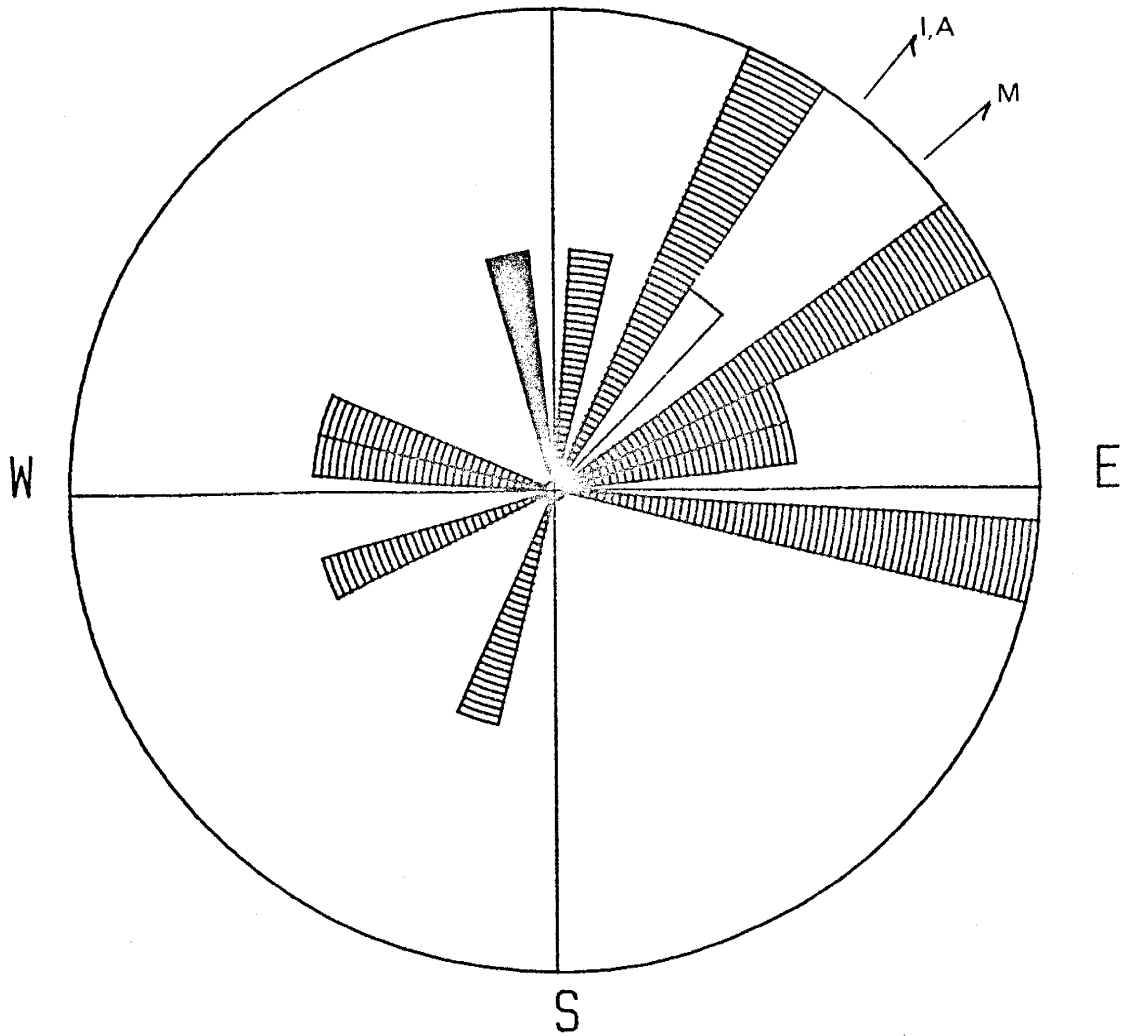
NUMBER OF VALUES: 22
 VECTOR MEAN: 242.03
 RESULTANT: 10.70
 VECTOR STRENGTH: 0.49

FREQUENCY TABULATION

SECTOR	FREQUENCY
5- 14	0
15- 24	0
25- 34	0
35- 44	0
45- 54	0
55- 64	0
65- 74	0
75- 84	0
85- 94	0
95-104	0
105-114	0
115-124	0
125-134	0
135-144	0
145-154	0
155-164	1
165-174	3
175-184	0
185-194	3
195-204	2
205-214	1
215-224	0
225-234	1
235-244	0
245-254	0
255-264	1
265-274	0
275-284	2
285-294	2
295-304	1
305-314	2
315-324	0
325-334	0
335-344	2
345-354	1
355- 4	0

Table H.

CHANNEL SAND
N



LEGEND




DATAFILE =	AS45
NO. MEASUREMENTS =	15
VECTOR MEAN =	38.9
VECTOR STRENGTH =	0.41
RADIUS =	2 MEASUREMENTS
	LARGE SCALE PALEOCURRENTS
	MEDIUM SCALE PALEOCURRENTS
	SMALL SCALE PALEOCURRENTS

Figure I.

LITHOLOGIC UNIT = AS45
 ORIGINAL AND ROTATED DATA

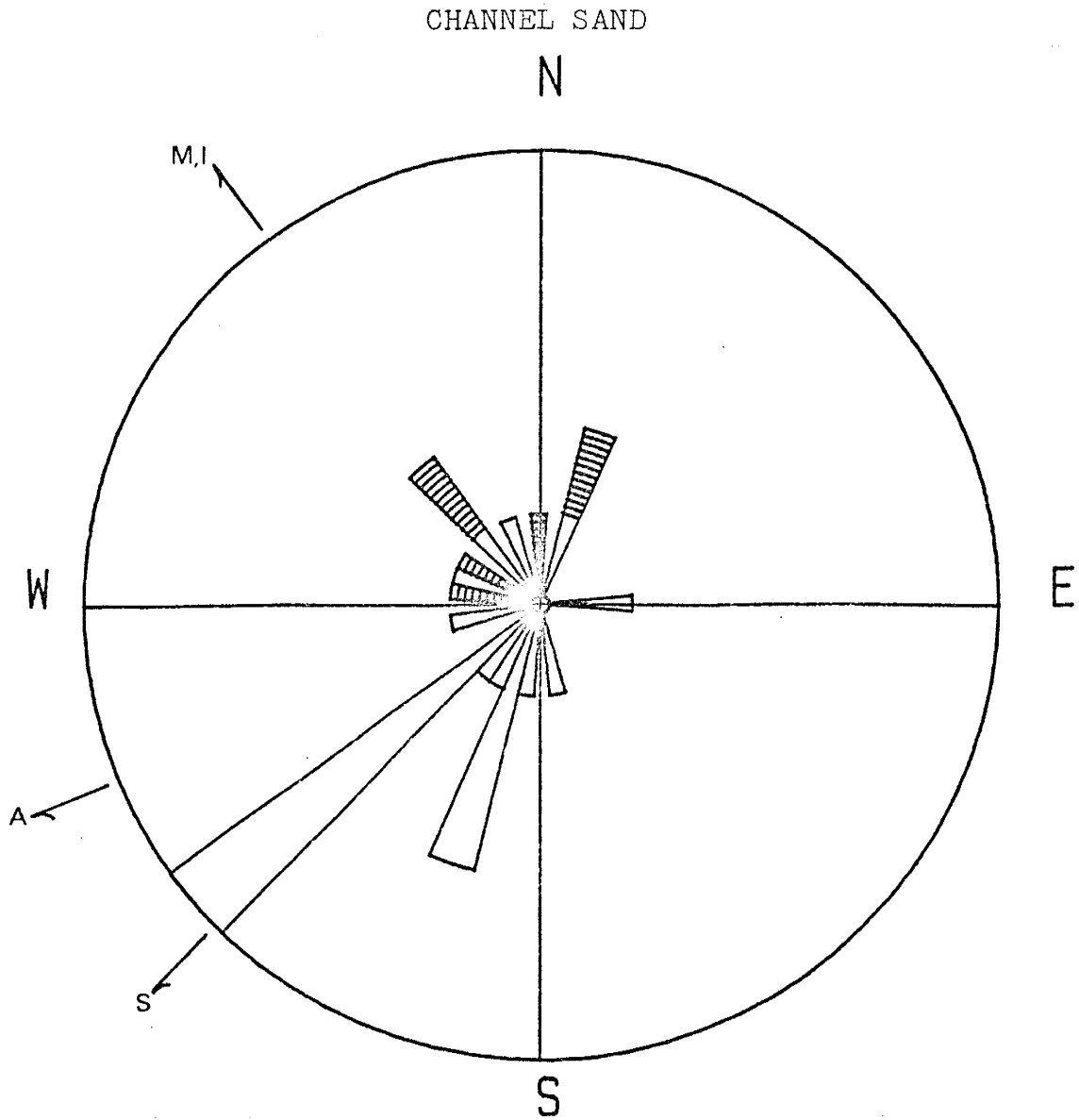
	DIRECTION	ORIGINAL DATA		TYPE	CORRECTED AZIMUTH
		AZIMUTH	INCLINATION		
REGIONAL:	S 30 E	150	15		
CURRENT BEDDING:	N 53 E	53	25	2	26
	S 75 E	105	20	2	58
	N 70 E	70	25	1	38
	S 20 E	160	13	2	285
	S 65 E	115	20	2	68
	S 40 E	140	18	2	101
	S 45 E	135	20	2	100
	S 20 W	200	12	2	278
	S 85 E	95	15	2	33
	S 40 E	140	10	3	348
	S 15 E	165	20	2	199
	S 15 E	165	15	2	247
	N 40 E	40	15	2	6
	S 50 E	130	18	2	78
REGIONAL:	S 30 W	210	15		
CURRENT BEDDING:	N 80 E	80	20	2	60

STATISTICAL SUMMARY:
 NUMBER OF VALUES: 15
 VECTOR MEAN: 38.89
 RESULTANT: 6.17
 VECTOR STRENGTH: 0.41

FREQUENCY TABULATION

SECTOR	FREQUENCY
5- 14	1
15- 24	0
25- 34	2
35- 44	1
45- 54	0
55- 64	2
65- 74	1
75- 84	1
85- 94	0
95-104	2
105-114	0
115-124	0
125-134	0
135-144	0
145-154	0
155-164	0
165-174	0
175-184	0
185-194	0
195-204	1
205-214	0
215-224	0
225-234	0
235-244	0
245-254	1
255-264	0
265-274	0
275-284	1
285-294	1
295-304	0
305-314	0
315-324	0
325-334	0
335-344	0
345-354	1
355- 4	0

Table I.



LEGEND

DATAFILE =	AS47
NO. MEASUREMENTS =	23
VECTOR MEAN =	247.8
VECTOR STRENGTH =	0.45
RADIUS =	5 MEASUREMENTS
<div style="display: inline-block; width: 15px; height: 15px; border: 1px solid black; background: repeating-linear-gradient(45deg, transparent, transparent 2px, black 2px, black 4px);"></div>	LARGE SCALE PALEOCURRENTS
<div style="display: inline-block; width: 15px; height: 15px; border: 1px solid black; background: repeating-linear-gradient(90deg, transparent, transparent 2px, black 2px, black 4px);"></div>	MEDIUM SCALE PALEOCURRENTS
<div style="display: inline-block; width: 15px; height: 15px; border: 1px solid black; background-color: white;"></div>	SMALL SCALE PALEOCURRENTS

Figure J.

LITHOLOGIC UNIT = AS47
 ORIGINAL AND ROTATED DATA

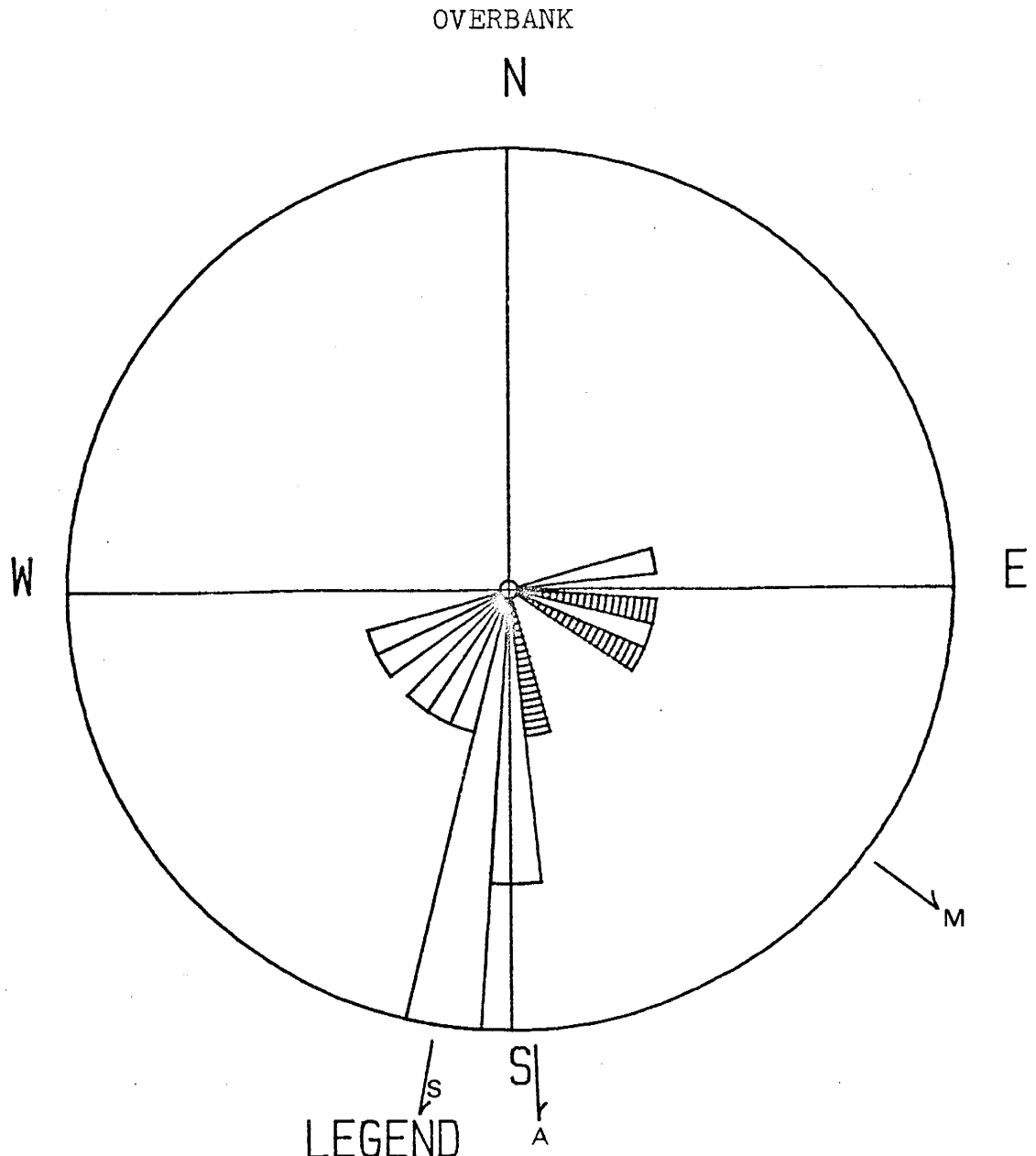
	DIRECTION	ORIGINAL DATA		TYPE	CORRECTED AZIMUTH
		AZIMUTH	INCLINATION		
REGIONAL:	S 10 W	190	5		
CURRENT BEDDING:	S 80 W	260	5	1	315
	N 50 W	310	5	1	340
	N 30 E	30	10	2	23
	S 20 W	200	5	1	286
	S 20 E	160	5	1	85
	N 10 W	350	15	2	355

DIRECTION	ORIGINAL DATA		TYPE
	AZIMUTH	INCLINATION	
S 40 W	220	0	1
S 15 W	195	0	1
S 10 E	170	0	1
S 45 W	225	0	1
S 20 W	200	0	1
N 20 E	20	0	1
S 45 W	225	0	1
N 65 W	295	15	2
S 45 W	225	5	1
N 40 W	320	10	2
S 20 W	200	0	1
S 80 W	260	0	1
S 50 W	230	5	1
N 85 W	275	10	2
S 30 W	210	0	1
S 10 W	190	0	1
S 45 W	225	0	1

STATISTICAL SUMMARY:
 NUMBER OF VALUES: 23
 VECTOR MEAN: 247.60
 RESULTANT: 10.36
 VECTOR STRENGTH: 0.45

FREQUENCY TABULATION	
SECTOR	FREQUENCY
5- 14	0
15- 24	2
25- 34	0
35- 44	0
45- 54	0
55- 64	0
65- 74	0
75- 84	0
85- 94	1
95-104	0
105-114	0
115-124	0
125-134	0
135-144	0
145-154	0
155-164	0
165-174	1
175-184	0
185-194	1
195-204	3
205-214	1
215-224	1
225-234	5
235-244	0
245-254	0
255-264	1
265-274	0
275-284	1
285-294	1
295-304	1
305-314	0
315-324	2
325-334	0
335-344	1
345-354	0
355- 4	1

Table J.



DATAFILE =	AS410
NO. MEASUREMENTS =	15
VECTOR MEAN =	177.4
VECTOR STRENGTH =	0.68
RADIUS =	3 MEASUREMENTS
LARGE SCALE PALEOCURRENTS	
MEDIUM SCALE PALEOCURRENTS	
SMALL SCALE PALEOCURRENTS	

Figure K.

LITHOLOGIC UNIT = AS410

		ORIGINAL DATA		
DIRECTION		AZIMUTH	INCLINATION	TYPE
S	0 W	180	0	1
S	5 W	185	0	1
S	70 W	250	0	1
N	80 E	80	0	1
S	85 E	95	15	2
S	25 W	205	0	1
S	35 W	215	0	1
S	20 W	200	0	1
S	10 W	190	0	1
S	10 E	170	10	2
S	60 W	240	0	1
S	70 E	110	0	1
S	60 E	120	10	2
S	10 W	190	0	1
S	5 E	175	0	1

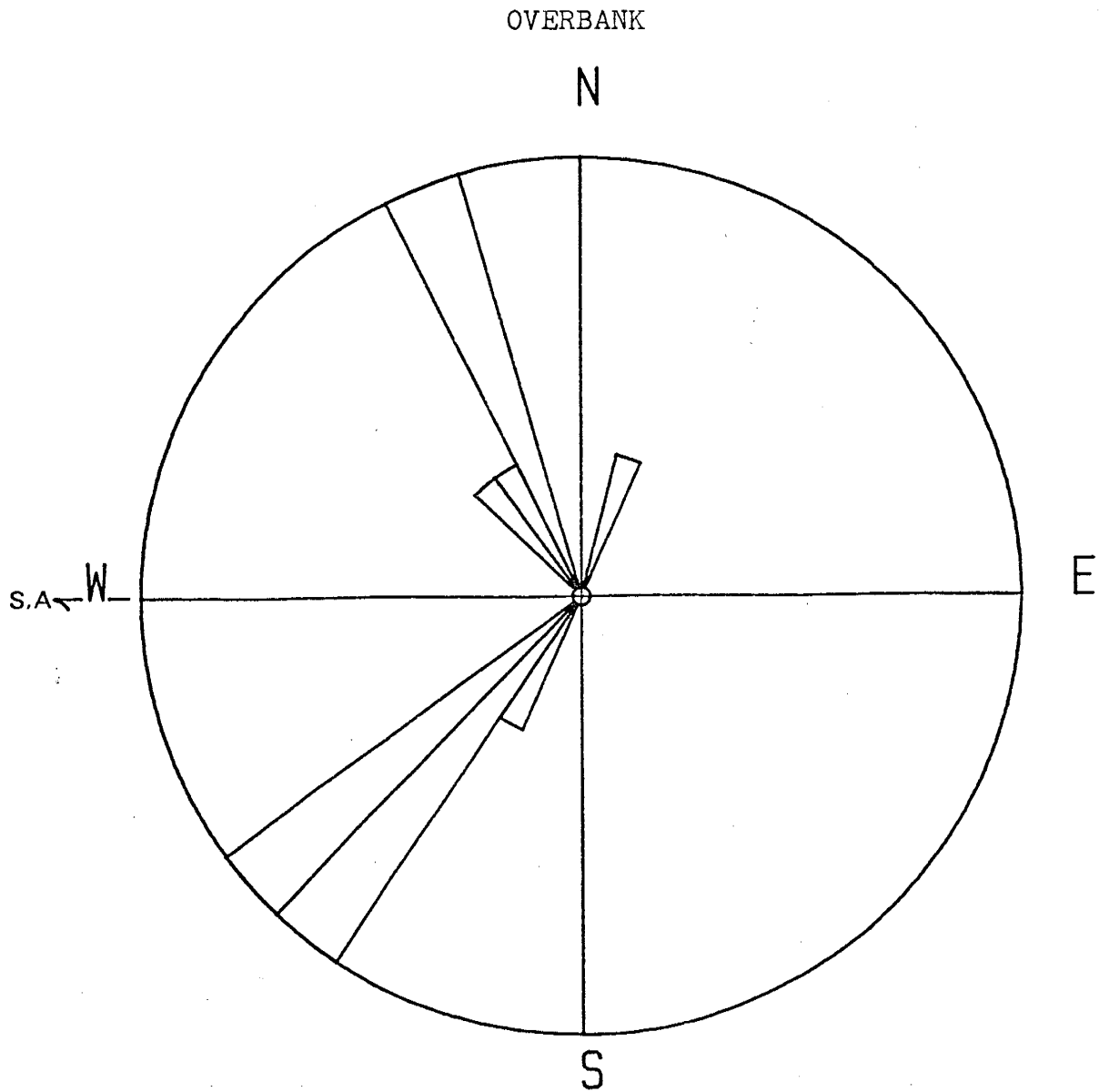
STATISTICAL SUMMARY:

NUMBER OF VALUES: 15
 VECTOR MEAN: 177.37
 RESULTANT: 10.22
 VECTOR STRENGTH: 0.68

FREQUENCY TABULATION

SECTOR	FREQUENCY
5- 14	0
15- 24	0
25- 34	0
35- 44	0
45- 54	0
55- 64	0
65- 74	0
75- 84	1
85- 94	0
95-104	1
105-114	1
115-124	1
125-134	0
135-144	0
145-154	0
155-164	0
165-174	1
175-184	2
185-194	3
195-204	1
205-214	1
215-224	1
225-234	0
235-244	1
245-254	1
255-264	0
265-274	0
275-284	0
285-294	0
295-304	0
305-314	0
315-324	0
325-334	0
335-344	0
345-354	0
355- 4	0

Table K.



LEGEND

DATAFILE =	AS412
NO. MEASUREMENTS =	13
VECTOR MEAN =	270.2
VECTOR STRENGTH =	0.51
RADIUS =	3 MEASUREMENTS
LARGE SCALE PALEOCURRENTS	
MEDIUM SCALE PALEOCURRENTS	
SMALL SCALE PALEOCURRENTS	

Figure L.

LITHOLOGIC UNIT = AS412

		ORIGINAL DATA		
DIRECTION		AZIMUTH	INCLINATION	TYPE
N	35 W	325	0	1
N	20 E	20	0	1
S	40 W	220	0	1
S	40 W	220	0	1
N	20 W	340	0	1
N	45 W	315	0	1
S	50 W	230	0	1
N	25 W	335	0	1
N	20 W	340	0	1
S	30 W	210	0	1
S	37 W	217	0	1
S	45 W	225	0	1
S	48 W	228	0	1

STATISTICAL SUMMARY:

NUMBER OF VALUES: 13
 VECTOR MEAN: 270.24
 RESULTANT: 6.65
 VECTOR STRENGTH: 0.51

FREQUENCY TABULATION

SECTOR	FREQUENCY
5- 14	0
15- 24	1
25- 34	0
35- 44	0
45- 54	0
55- 64	0
65- 74	0
75- 84	0
85- 94	0
95-104	0
105-114	0
115-124	0
125-134	0
135-144	0
145-154	0
155-164	0
165-174	0
175-184	0
185-194	0
195-204	0
205-214	1
215-224	3
225-234	3
235-244	0
245-254	0
255-264	0
265-274	0
275-284	0
285-294	0
295-304	0
305-314	0
315-324	1
325-334	1
335-344	3
345-354	0
355- 4	0

Table L.

BIBLIOGRAPHY

- Allen, J.R.L., 1966, On bed forms and paleocurrents:
Sedimentology, v.6, pp.151-190.
- Baars, D.L., 1961, Permian strata of central New Mexico:
New Mexico Geol.Soc.Guidebook, 12th field conference,
p. 113-120.
- Bachman, G.O., 1968, Geology of the Mockingbird Gap
Quadrangle, Lincoln and Socorro Counties, New Mexico:
U.S. Geol. Survey Prof. Pap. 594-J, 43 p.
- , 1964, Southwestern edge of the Paleozoic landmass
in southwestern New Mexico: New Mexico Geol.Soc.
Guidebook, 15th field conference, p.70-72.
- Cappa, J.A. and MacMillan, J.R., 1983, Paleocurrent
Analysis of Early Permian Abo Formation, Cerros de
Amado area, Socorro County, New Mexico: New Mexico
Geol.Soc. Guidebook, 34th field conference, p.15-16.
- Darton, N.H., 1928, "Red Beds" and associated formations
in New Mexico: U.S.Geol.Survey Bull.794, 356 p.

- Daut, S., 1978, Paleocurrent computer program, Iowa Geological Survey.
- Dixon, W.J., and Massey, F.J.Jr., 1957, Introduction to statistical analysis, 2nd ed., New York, McGraw-Hill Book Co.488 p.
- Durand, D., and Greenwood, J.A., 1958, Modifications of the Rayleigh test for Uniformity in analysis of two dimensional orientation data: Journal of Geology, v.66, no.3, pp. 229-238.
- Griffiths, J.C.and Rosenfeld, M.A., 1953, A further test of dimensional orientation of Quartz grains in Bradford sand: Am.Jour.Sci., v.251, p.192-214.
- Gumbel, E.J., Greenwood, J.A., and Durand, D., 1953, The circular normal distribution: theory and tables: Jour.Am. Stat.Assoc., v.48, p.131-152.
- Harrison, P.W., 1957, New Techniques for three-dimensional fabric analysis of till and englacial debris containing particles from 3 to 40 millimeters: Jour.Geology, v.65, p. 98-105

- Hatchell, W.O.; Blagbrough, J.W., and Hill, J.M.,
1982, Stratigraphy and copper deposits of the Abo
Formation, Abo Canyon area, central New Mexico: New
Mexico Geol.Soc. Guidebook, 33rd field conference,
Albuquerque country II, pp. 249-260.
- High, L.R., and Picard, M.D., 1971, Mathematical
treatment of orientation data: (in) R.E.Carver
(editor), Procedures in sedimentary petrology: New
York, John Wiley and Sons Inc., p.21-44.
- Hunt, A., 1983, Plant fossils and lithostratigraphy of the
Abo Formation (lower Permian) in the Socorro area and
plant biostratigraphy of Abo red beds in New Mexico:
New Mexico Geol. Soc. Guidebook, 34th Field
Conference, Socorro region II, pp. 157-163
- Jones, T.A., 1968, Statistical Analysis of Orientation
data: Journal of Sedimentary Petrology, v.38, no.1,
pp. 61-67.
- King, R.E., 1945, Stratigraphy and Oil producing Zones of
the Pre-San Andres Formations of southeastern New
Mexico: New Mexico School of Mines, State Bureau Mines
and Min. Res., Bull.23, 34 p.

Kottowski, F.E., and Stewart, W.J., 1970, The Wolfcampian Joyita uplift in central New Mexico: New Mexico Institute of Mining and Technology, State Bureau Mines and Min.Res., Memoir 23, part 1, p.1-31.

LaPoint, D., 1974, Possible source areas for sandstone copper deposits in Northern New Mexico: New Mexico Geol. Soc. Guidebook, 25th Field conference, p.305-307.

Lee, W.T., and Girty, G.H., 1909, The Manzano group of the Rio Grande valley of New Mexico: U.S. Geol. Survey Bull. 389, 141 p.

Leopold, L.B., and Maddock, T.Jr., 1953, The Hydraulic geometry of stream channels and some physiographic implications: U.S. Geol. Survey Prof. Paper 252, 57 p.

Leopold, L.B., and Wolman, M.G., 1960, River meanders: Geol. Soc. America Bull., v.71, p.769-794.

McKee, E.D., 1967, Paleotectonic investigations of the Permian system in the United States - Arizona and Western New Mexico: U.S. Geol. Survey Prof. Paper 515, p.203-223.

McKee, E.D., and Weir, G.W., 1953, Terminology for stratification and cross-stratification in sedimentary rocks: Geol.Soc.Amer.Bull., v.64, pp.381-390.

Meyer, R.F., 1966, Geology of the Pennsylvanian and Wolfcampian rocks in southeastern New Mexico: New Mexico Institute of Mining and Technology, State Bureau Mines and Min.Res., Memoir 17, 123 p.

Miller, R.L., and Kahn, J.S., 1962, Statistical analysis in the geological sciences: New York, John Wiley and Sons (publishers) 483 p.

Myers, D.A., 1977, Geologic map of the Scholle Quadrangle, Socorro, Valencia and Torrance counties, New Mexico: U.S. Geological Survey Geologic Quadrangle Map GQ-1412.

Needham, C.E., and Bates, R.L., 1943, Permian type sections in central New Mexico: Geol.Soc.Amer.Bull., v.54, p.1653-1667.

Northrup, S.A., and Wood, G.H., 1946, Geology of Nacimiento Mountains, San Pedro Mountain and adjacent plateaus in

parts of Sandoval and Rio Arriba Counties, New Mexico:
U.S. Geol. Survey Oil and Gas preliminary
investigations map 57.

Otte, C.Jr., 1959, Late Pennsylvanian and Early Permian
stratigraphy of the northern Sacramento mountains,
Otero county, New Mexico: New Mexico Institute Mining
and Technology, State Bureau Mines and Min.Res.,
Bull.50, 111 p.

Pettijohn, F.J., Potter, P.E., Siever, R., 1973, Sand
and Sandstone: Springer-Verlag (publishers), p.332.

Phillips, F.C., 1954, the use of the stereographic
projection in structural geology: London, Edwin Arnold
(publishers) Ltd., 86 p.

Pray, L.C., 1961, Geology of the Sacramento Mountains
escarpment, Otero County, New Mexico: New Mexico
Institute Mining and Technology, State Bureau Mines and
Min.Res., Bull.35, 144 p.

Rayleigh, Lord (Strutt, J.W.), 1894, The theory of sound:
2nd ed., v.1, 480 p., New York, reprinted in 1945 by
Dover Publications.

Reiche, P., 1938, An analysis of cross lamination: Cocino Sandstone: Jour.Geol., v.46, p.905-932.

Schumm, S.A., 1963, Sinuosity of Alluvial rivers on the Great Plains: Geol.Soc.Amer.Bull., v.74, p.1089-1100

-----, 1972, Fluvial paleochannels: (in) J.K.Rigby and W.K.Hamblin (editors), Recognition of ancient sedimentary environments: Soc.Econ.Paleontologist and Mineralogists: Spec.Pub.16, p.98-107.

Thompson, M.L., 1942, Pennsylvanian System in New Mexico: New Mexico School of Mines, State Bureau of Mines and Mineral Resources, bulletin no. 17, p. 20.

Tonking, W.H., 1957, Geology of the Puertocito quadrangle, Socorro County, New Mexico: New Mexico Institute Mining and Technology, State Bureau Mines and Min.Res., Bull.41, 67 p.

Van De Graaf, F.R., 1972, Fluvial-Deltaic Facies of the Castlegate Sandstone (Cretaceous), East-Central Utah: Journal of Sed.Pet., v.42, no.3, p.558-571.

Watson, G.S. and Williams, E.J., 1956, On the construction

(91)

of significance tests on the circle and the sphere:
Biometrika, v.43, p.344-352.

Wilpolt, R.H., and Waneck, A.A., 1951, Geology of the
region from Socorro and San Antonio east to Chupadera
Mesa, Socorro County, New Mexico: U.S.Geol.Survey, Oil
and Gas Invest.Map, OM 121.